Superconducting Nanowire Single-Photon Detector as a Key Element for Quantum Photonic Integrated Circuits

Gregory N. Goltsman

Moscow State Pedagogical University

Korneev Alexander
Kovalyuk Vadim
An Pavel
Voronov Boris

Karlsruhe Institute of Technology (KIT)

University of Münster, Germany

Pernice Wolfram H.P.
Kahl Oliver
Ferrari Simone
Vetter Andrea

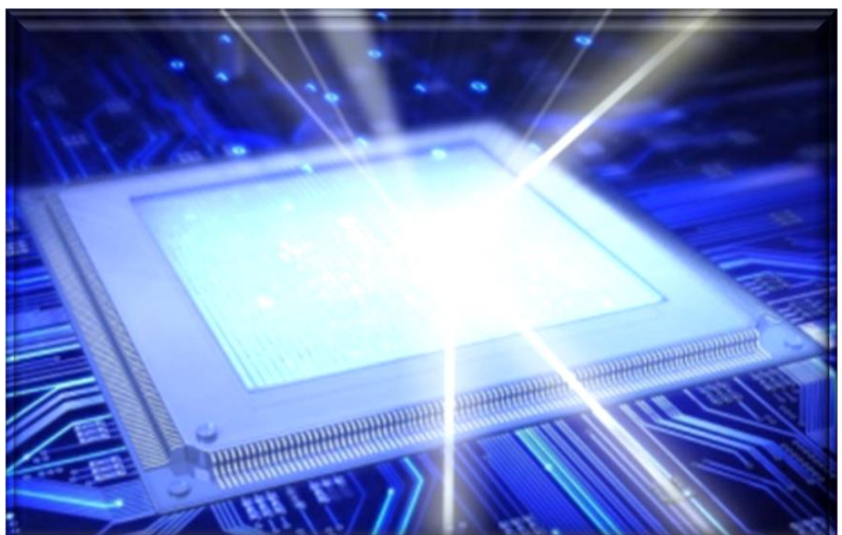

EUCAS 2017, Geneva, 20 September 2017

Outline:

1. Introduction: Superconducting single photon detector (SSPD) – from first idea to commercially available devices and systems
2. Travelling Wave Single-Photon Detector With Near-Unity Quantum Efficiency – superconducting stripe on optical waveguide
3. Silicon Nitride on Si - Single-photon platform for the realization of Quantum-Photonic Integrated Circuits (QPICs)
4. Other material platforms for integrated quantum photonics: Si, III-V semiconductors, Bulk diamond and diamond-on-insulator
5. Single-photon platform for the realization of Quantum-Photonic Integrated Circuits (QPICs)
6. The technology is scalable on Si chip and includes grating couplers, beam splitters, MZ interferometers, etc.
7. Fully integrated quantum photonic circuit with an electrically driven light sources - waveguide-coupled semiconducting single-walled carbon nanotubes
8. On-chip spectrometer: arrayed waveguide grating and SSPDs.
9. On-chip heterodyne receiver based on SSPD mixer with ultralow local oscillator power
10. Conclusions

First observation of SSPD response and first idea of device physics

Picosecond superconducting single-photon optical detector

APPLIED PHYSICS LETTERS VOLUME 79, NUMBER 6 6 AUGUST 2001

G. N. Gol'tsman,[a] O. Okunev, G. Chulkova, A. Lipatov, A. Semenov, K. Smirnov, B. Voronov, and A. Dzardanov

Department of Physics, Moscow State Pedagogical University, Moscow 119435, Russia

C. Williams and Roman Sobolewski[b]

Department of Electrical and Computer Engineering and Laboratory for Laser Energetics, University of Rochester, Rochester, New York 14627-0231

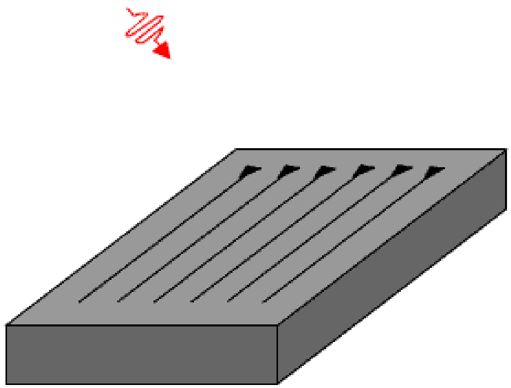

FIG. 1. Schematics of the supercurrent-assisted hotspot formation mechanism in an ultrathin and narrow superconducting strip, kept at temperature far below T_C are shown. The arrows indicate direction of the supercurrent flow.

Quantum detection by current carrying superconducting film

Physica C 351 (2001) 349–356

Alex D. Semenov [*,1], Gregory N. Gol'tsman, Alexander A. Korneev

Department of Physics, State Pedagogical University of Moscow, 11989 Moscow, Russian Federation

PHYSICA C
www.elsevier.nl/locate/physc
ELSEVIER
Received 18 July 2000; received in revised form 9 October 2000; accepted 11 October 2000

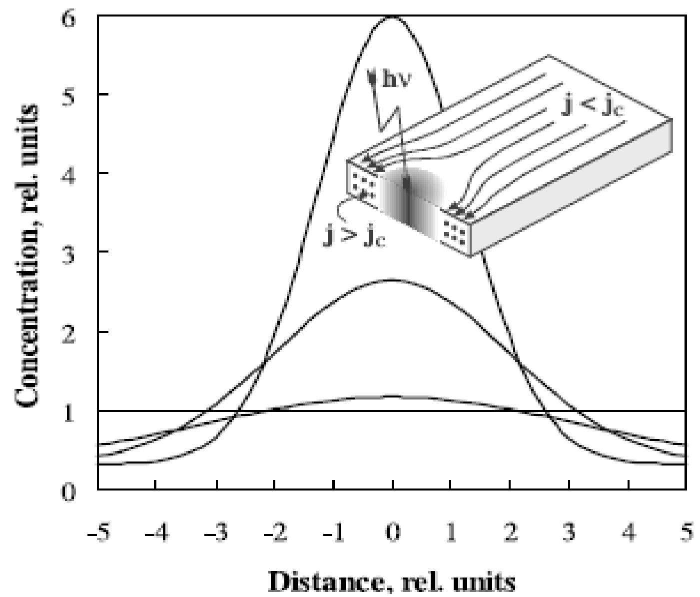

Fig. 1. Concentration of nonequilibrium quasiparticles across the width of the film at different moments after the photon has been absorbed. Time delays are 0.8, 2.0 and 5.0 measured in units of the thermalization time. Distance from the absorption site is shown in units of the thermalization length. Inset illustrates redistribution of supercurrent in the superconducting film with the normal spot – the basis of quantum detection. It shows the cross-section of the film drawn through the point where photon has been absorbed.

High quality ultrathin superconducting NbN film is one of the best practical material for SSPD

NbN on 3C-SiC buffer layer on Si substrate (HREM)

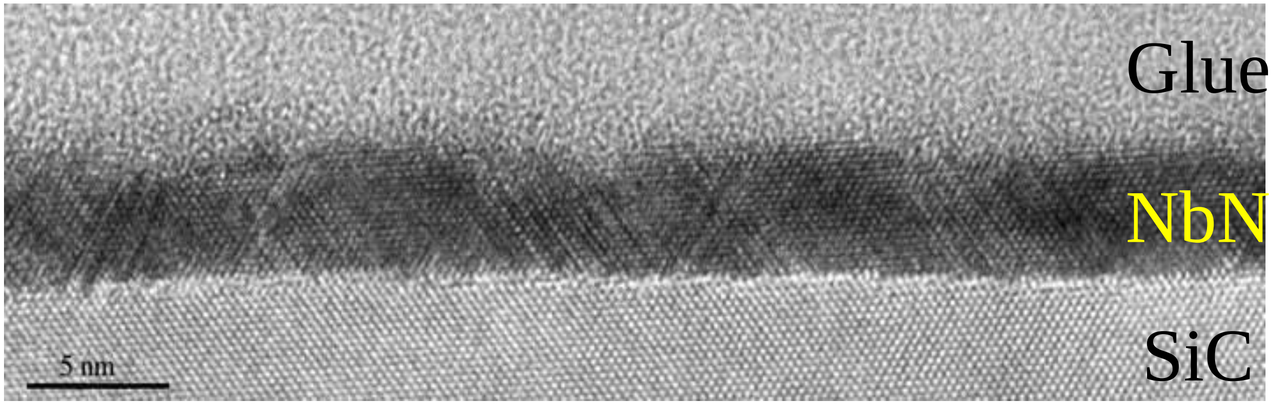

NbN is monocrystalline
a_0 (3C-SiC) =4.36Å
a_0 (NbN) =4.39Å
Thickness is 3.5 – 4.1 nm
Not really flat surface

NbN on Si substrate

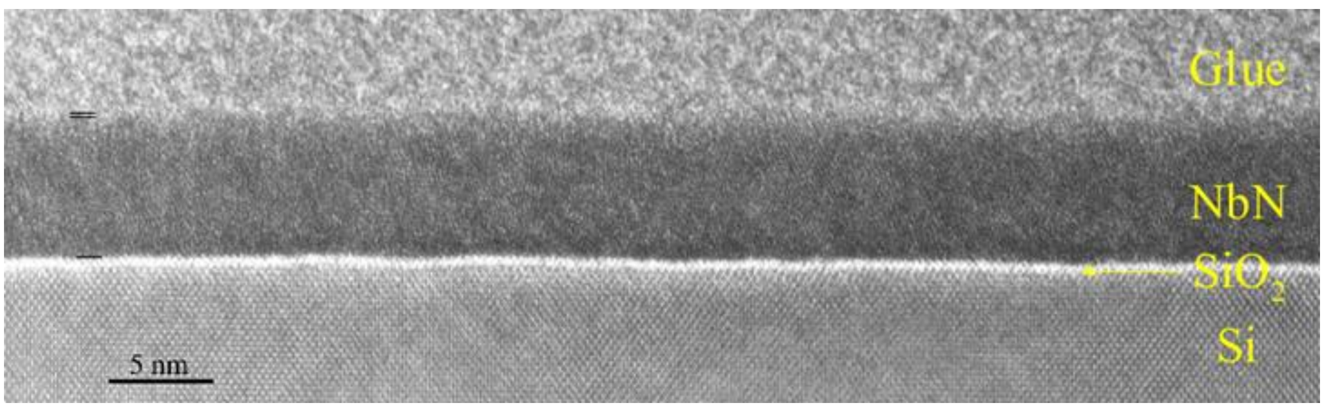

The NbN on Si is polycrystalline.

Gao, J.R., Hajenius, M., Tichelaar, F.D., Klapwijk, T.M., Voronov, B., Grishin, E., Goltsman, G., Zorman, C.A., Mehregany, M. Monocrystalline NbN nanofilms on a 3C-SiCSi substrate, APL, 91 (6), 2007.

First Implementation of NbN SSPD: Silicon CMOS IC Device Debug OptiCA® System with NbN SSPD commercialized by NPTest, Inc.

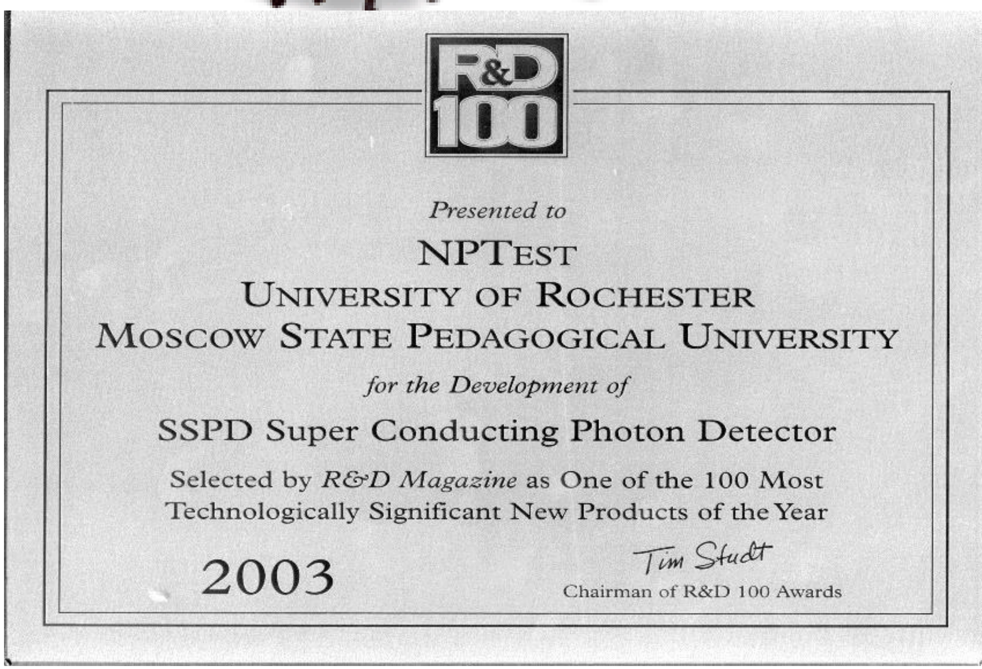
R&D 100

Presented to

NPTest
University of Rochester
Moscow State Pedagogical University

for the Development of

SSPD Super Conducting Photon Detector

Selected by *R&D Magazine* as One of the 100 Most Technologically Significant New Products of the Year

2003

Tim Studt
Chairman of R&D 100 Awards

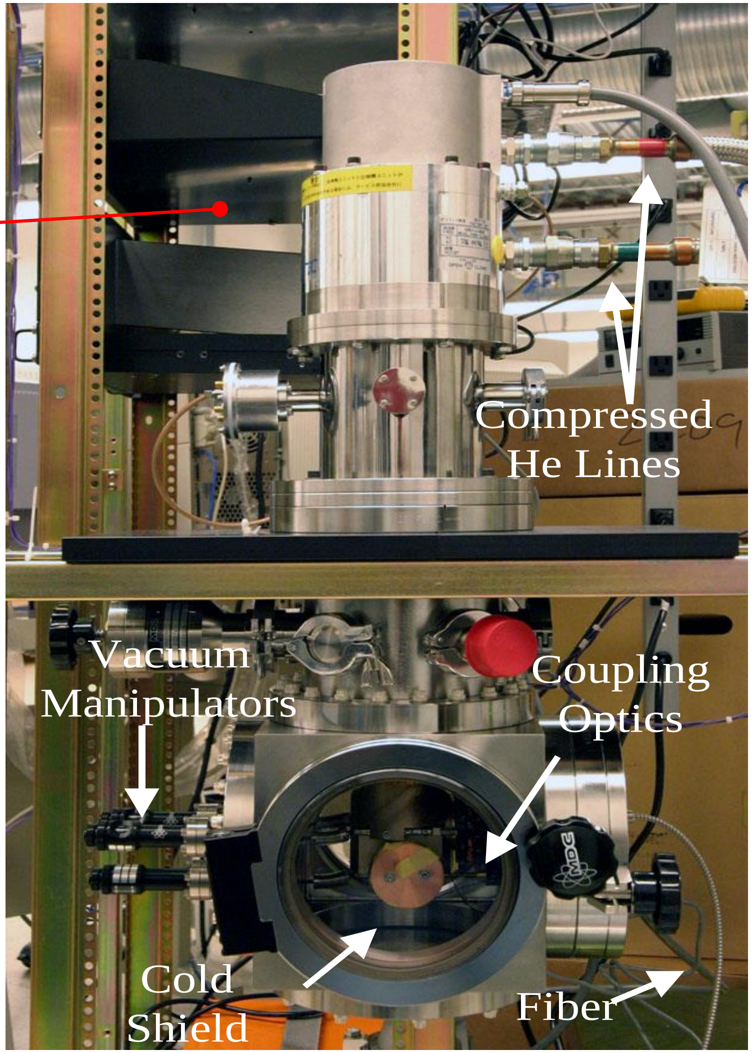

Normally operating nMOS transistor emits near IR photons (0.9-1.4um) when current passes through the channel. Time-correlated photon emission detection measures transistor switching time.

Practical single-photon receiver based on SSPD

Now: Quantum efficiency 80% at 1550nm, jitter 20ps, max. counting rate 100 MHz and dark count rate $10 s^{-1}$

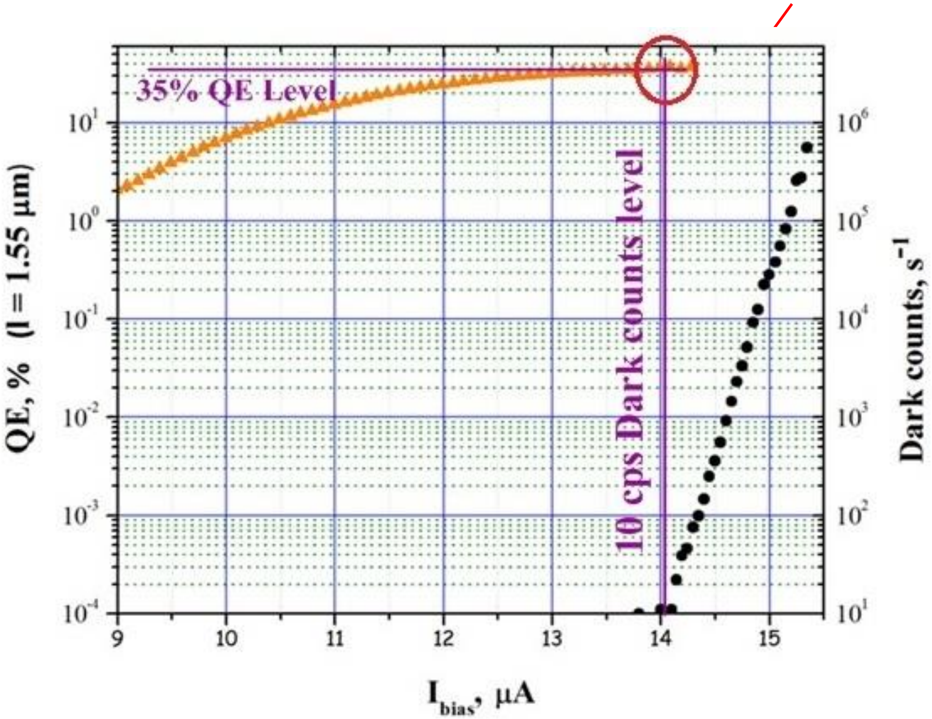

Cavity-integrated SSPD

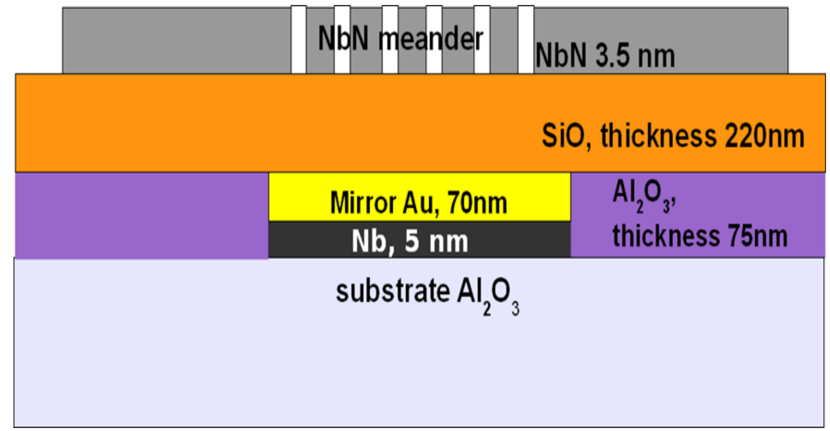

Spectral range	Quantum efficiency (referred to optical input)
0.7 – 1.3 μm	85 %
1.3 – 1.6 μm	80 %
1.6 – 2.3 μm	50 %

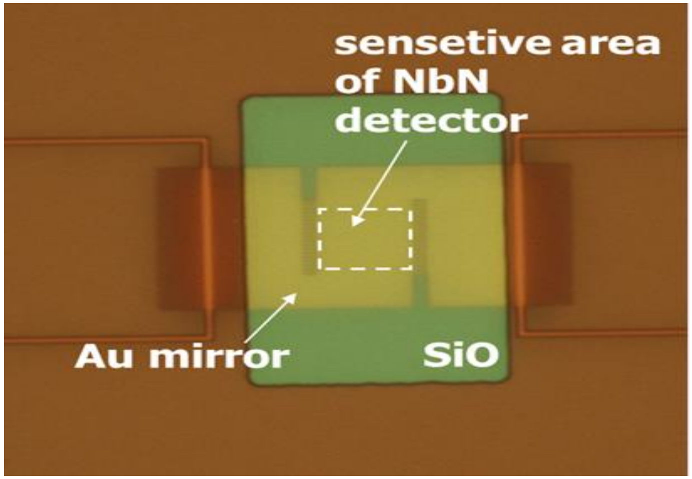

High Speed Travelling Wave Single-Photon Detectors With Near-Unity Quantum Efficiency W. Pernice, C. Schuck, O. Minaeva, M. Li, G. Goltsman, A. Sergienko, H. Tang, Nature Communications, 3, 1325 (2012)

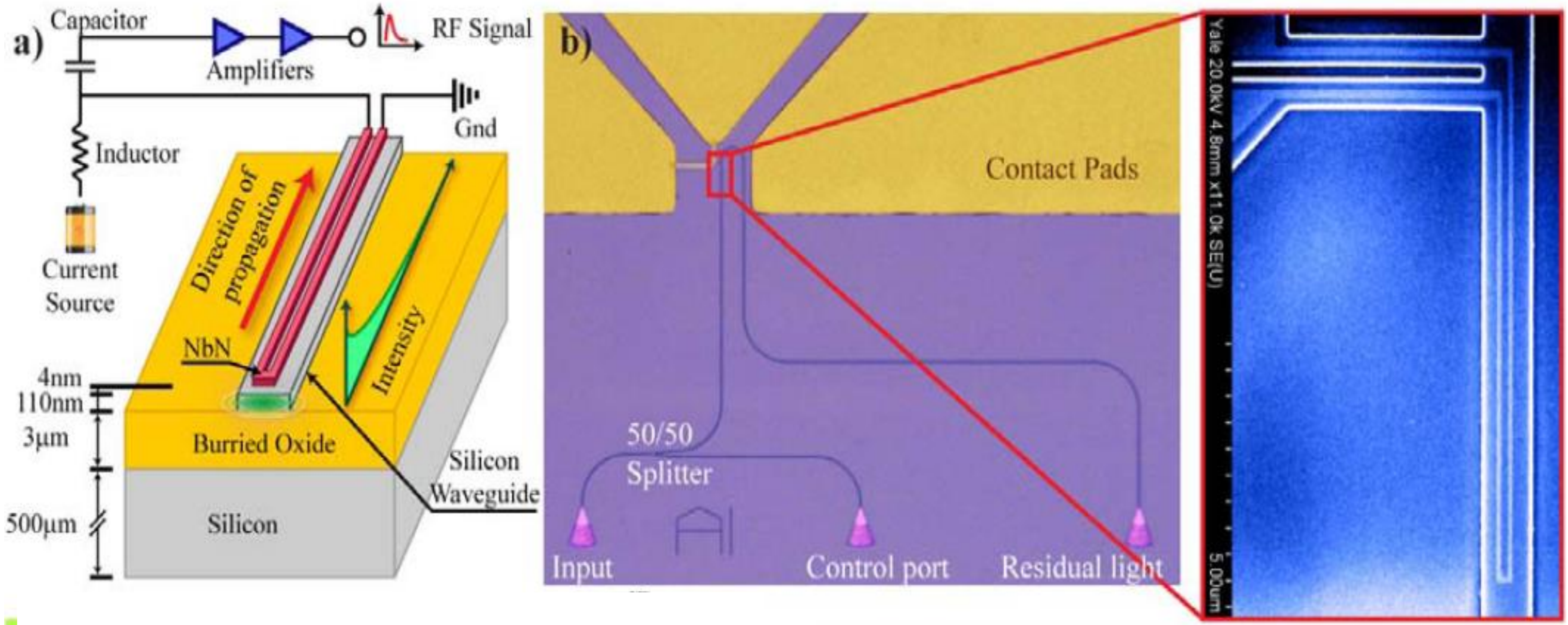

a) Principle of the travelling wave SSPD: a sub-wavelength absorbing NbN nanowire is patterned atop a silicon waveguide to detect single photons; Max. QE= 91%
b) Optical micrograph of a fabricated device showing the optical input circuitry, RF contact pads and the SSPD; Inset: zoom into the detector region with an SEM image showing the detector regime. The control and residual ports are used for calibration purposes.

Silicon Nitride on Si - Single-photon platform for the realization of integrated SSPD array

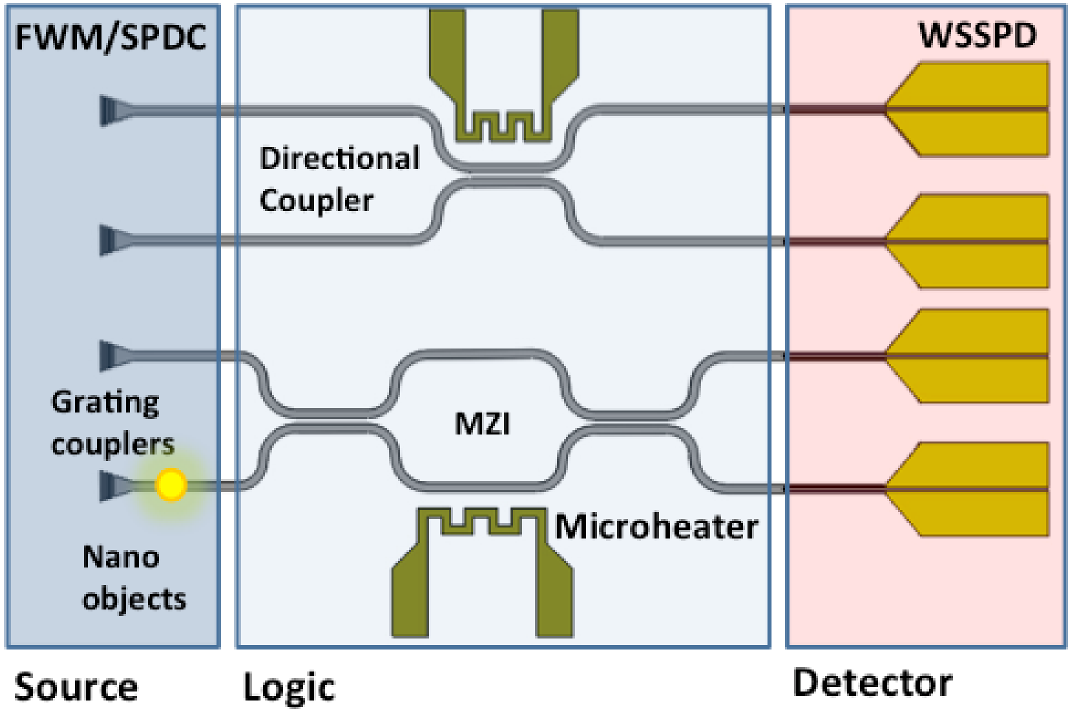

Why on-chip photonics?

- ✓ The ability to integrate a huge number of optical components in a small area,
- ✓ Superposition of quantum states can be easily represented, encrypted, transmitted and detected
- ✓ Easy to manipulate (Linear Optics Quantum computation(LOQC), using only linear optical elements: beam splitters, phase shifters and mirrors)
- ✓ Low power consumption

Why silicon nitride?

- ✓ Wide band gap → small absorption in visible and in IR range
- ✓ High refractive index
- ✓ Good mechanical properties
- ✓ Possibility to create SPS due to nonlinearity
- ✓ Compatibility with NbN thin film deposition process

Why WSSPD?

- ✓ Compact design
- ✓ High detection efficiency
- ✓ Low timing jitter
- ✓ Low dead time
- ✓ No gating needed
- ✓ No afterpulsing

Si-based platforms

a)

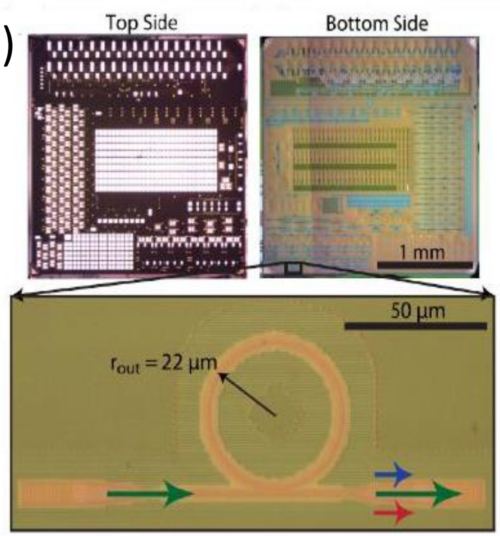

(a) Integration of a Si ring resonator on a 45 nm CMOS SOI chip [26].

b)

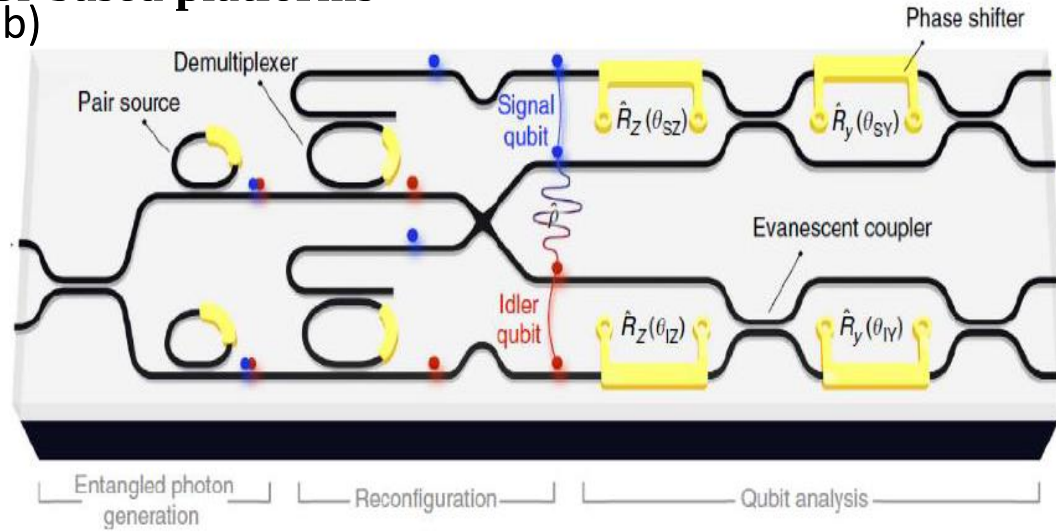

(b) On-chip generation and analysis of a two-photon entangled state [27]. Pump laser and detectors are external to the SOI chip.

c)

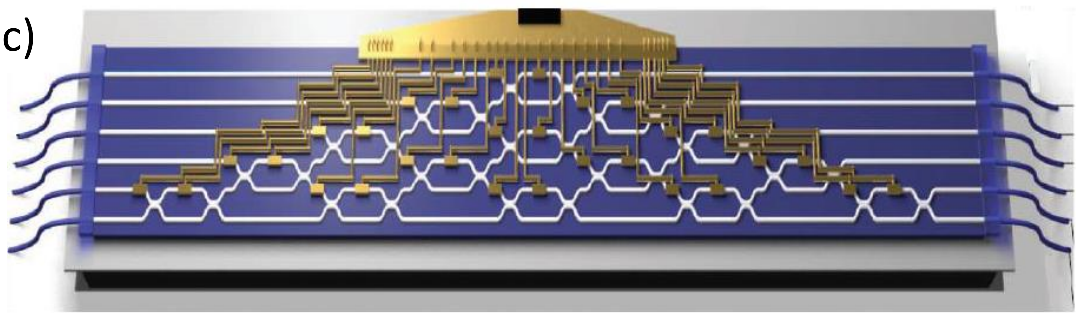

(c) A fully reconfigurable circuit made with silica waveguides capable of performing all linear optical operations possible for its size [28].

d)

(d) A micrograph showing a linear optical CNOT gate realized using silicon nitride-on-silica rib waveguides [29].

 [26] C. M. Gentry, J. M. Shainline, M. T. Wade, M. J. Stevens, S. D. Dyer, X. Zeng, F. Pavanello,T. Gerrits, S. W. Nam, R. P. Mirin, and M. A. Popović, Optica 2, 1065 (2015); [27] J. W. Silverstone, R. Santagati, D. Bonneau, M. J. Strain, M. Sorel, J. L. O’Brien, and M. G. Thompson, Nat. Commun. 6, 7948 (2015); [28] J. Carolan, C. Harrold, C. Sparrow, E. Martín-López, N. J. Russell, J. W. Silverstone, P. J. Shadbolt, N. Matsuda, M. Oguma, M. Itoh, G. D. Marshall, M. G. Thompson, J. C. F. Matthews, T. Hashimoto, J. L. O’Brien, and A. Laing, Science 349, 711 (2015); [29] M. Poot, C. Schuck, X. Ma, X. Guo, and H. X. Tang, Opt. Express **24**, 6843 (2016).

S. Bogdanov, M.Y. Shalaginov, A. Boltasseva, V.M. Shalaev, Opt. Mater. Express, 7, 111-132 (2017)
"Material platforms for integrated quantum photonics"

III-V semiconductors platforms

a)

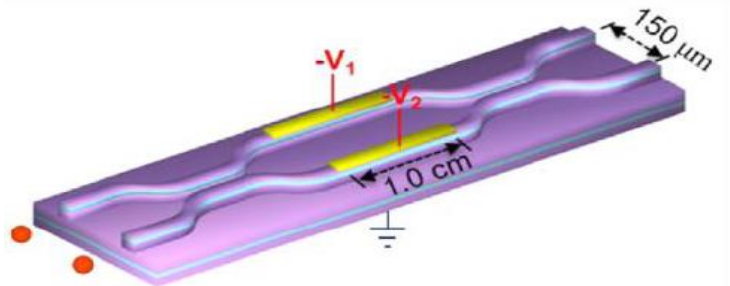

(a) Passive and active photonic elements realized using integrated GaAs waveguides [60].

c)

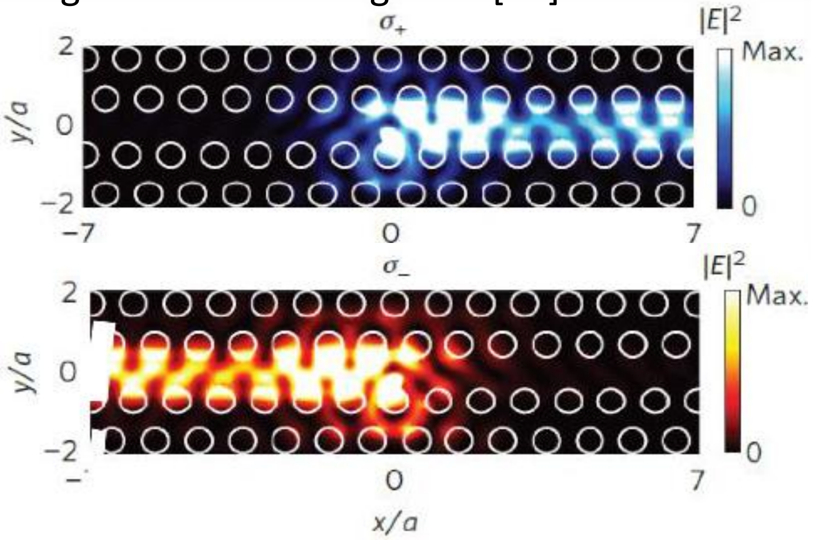

(c) Chiral photonic crystal waveguide realizing an efficient spin-photon interface with a quantum dot for the realization of deterministic two-photon gates [67].

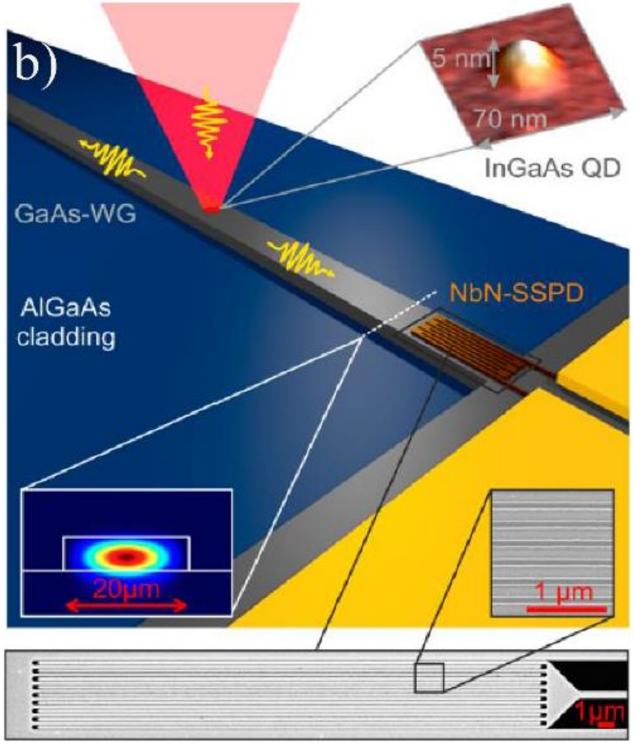

(b) A ridge waveguide structure, hosting a layer of GaAs/InGaAs QDs and an NbN-SSPD [66]. The fluorescence from a QD is collected by the waveguide and detected on chip. The simulated waveguide mode profile, an SEM image of the SNSPD and an AFM image of a QD are shown in insets.

[60] J. Wang, A. Santamato, P. Jiang, D. Bonneau, E. Engin, J. W. Silverstone, M. Lermer, J. Beetz, M. Kamp, S. Höfling, M. G. Tanner, C. M. Natarajan, R. H. Hadfield, S. N. Dorenbos, V. Zwiller, J. L. O'Brien, and M. G. Thompson, Opt. Commun. 327, 49 (2014); [66] G. Reithmaier, M. Kaniber, F. Flassig, S. Lichtmannecker, K. Müller, A. Andrejew, J. Vučković, R. Gross, and J. J. Finley, Nano Lett. 15, 5208 (2015); [67] I. Söllner, S. Mahmoodian, S. L. Hansen, L. Midolo, A. Javadi, G. Kiršanskė, T. Pregnolato, H. El-Ella, E. H. Lee, J. D. Song, S. Stobbe, and P. Lodahl, Nat. Nanotechnol. 10, 775 (2015).

S. Bogdanov, M.Y. Shalaginov, A. Boltasseva, V.M. Shalaev, Opt. Mater. Express, 7, 111-132 (2017)
"Material platforms for integrated quantum photonics"

Bulk diamond and diamond-on-insulator

a)

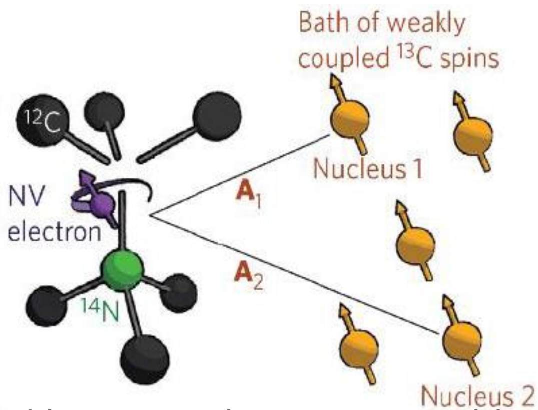

(a) Diamond lattice nuclear spins neighboring a single NV center (top) allow the realization of quantum error correction (bottom) [85].

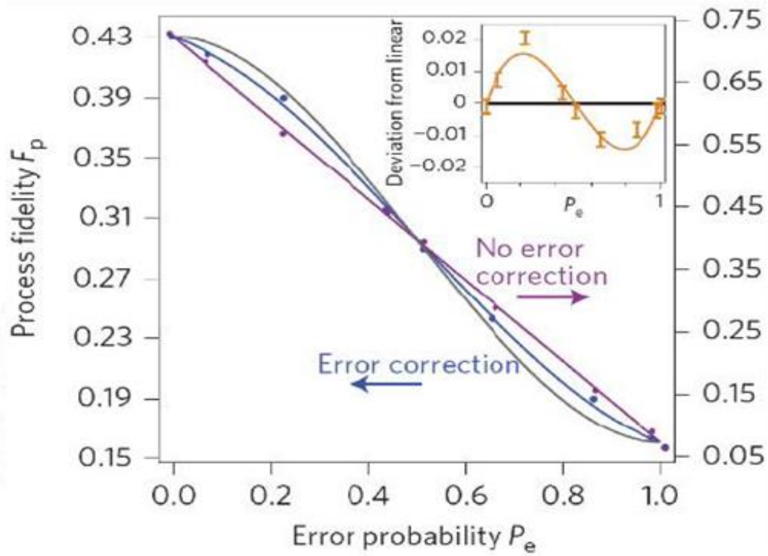

b)

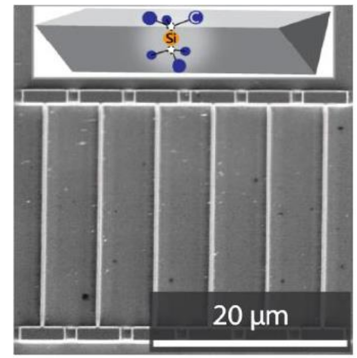

(b) Free-standing nanobeam diamond waveguides containing SiV centers with narrow inhomogeneous spectral distribution for scalable single-photon generation [88].

c)

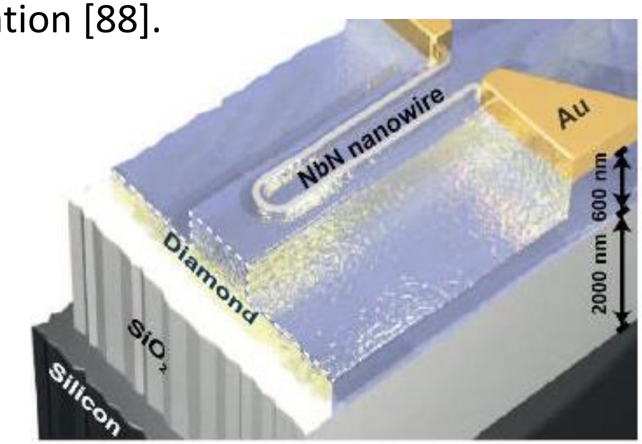

(c) NbN SNSPD integrated onto a diamond-on-insulator rib waveguide featuring an on-chip detection efficiency of 66% [89].

[85] T. H. Taminiau, J. Cramer, T. van der Sar, V. V Dobrovitski, and R. Hanson, Nat. Nanotechnol. 9, 171 (2014); [88] R. E. Evans, A. Sipahigil, D. D. Sukachev, A. S. Zibrov, and M. D. Lukin, Phys. Rev. Appl. 5, 44010 (2016); [89] P. Rath, O. Kahl, S. Ferrari, F. Sproll, G. Lewes-Malandrakis, D. Brink, K. Ilin, M. Siegel, C. Nebel, and W. Pernice, Light Sci. Appl. 4, e338 (2015).

SEM image of a fabricated waveguide circuits

SEM image of a fabricated nanophotonic circuit for balance measurements of an absorption coefficient

False colors of nanowire atop of waveguide with different width

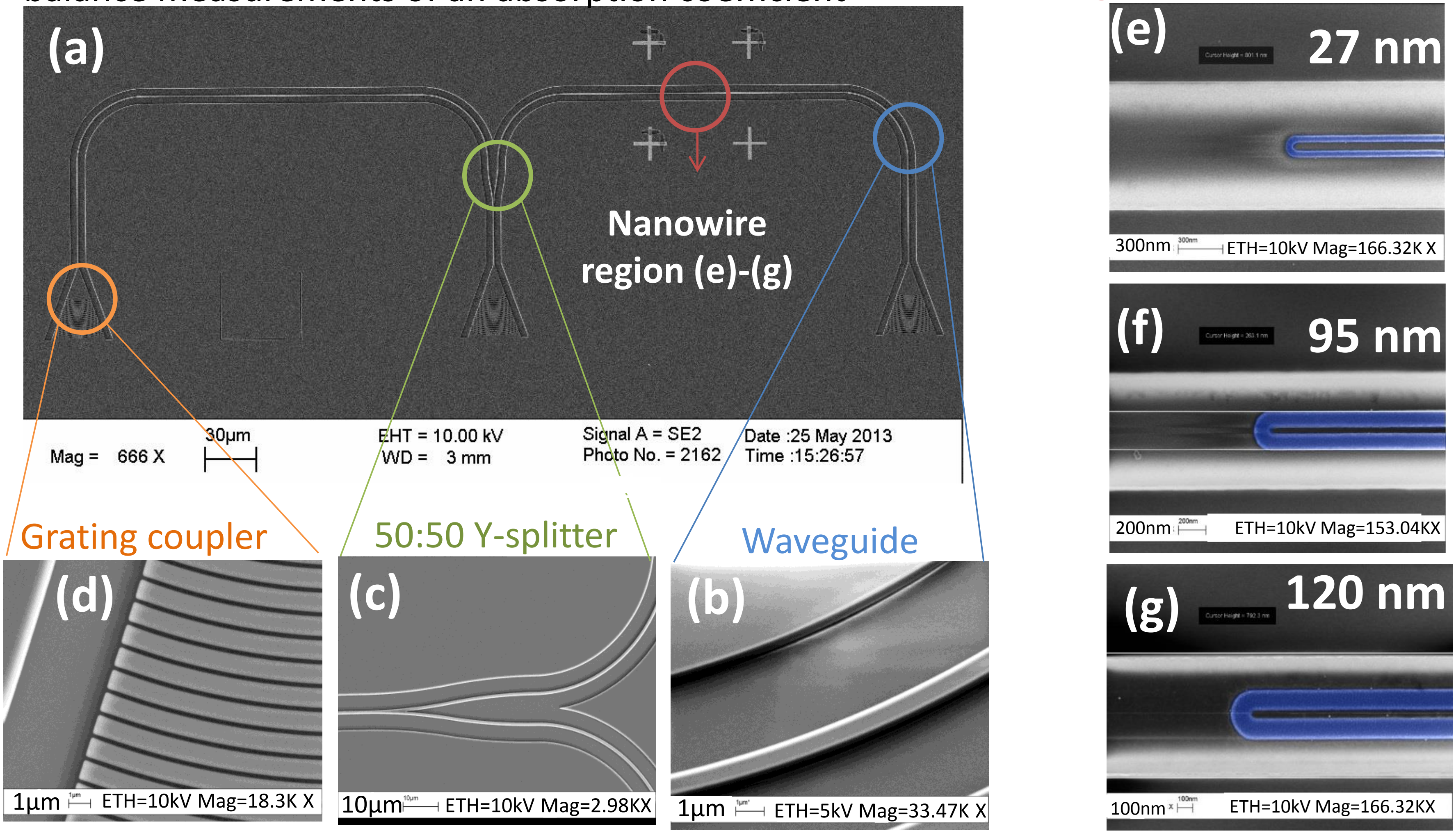

V. Kovalyuk, W. Hartmann, O. Kahl, N. Kaurova, A. Korneev, G. Goltsman, and W. H. P. Pernice, “Absorption engineering of NbN nanowires deposited on silicon nitride nanophotonic circuits,” *Opt. Express*, vol. 21, no. 19, pp. 22683–92, 2013.

Focusing grating coupler optimization

SEM image of (FGC)

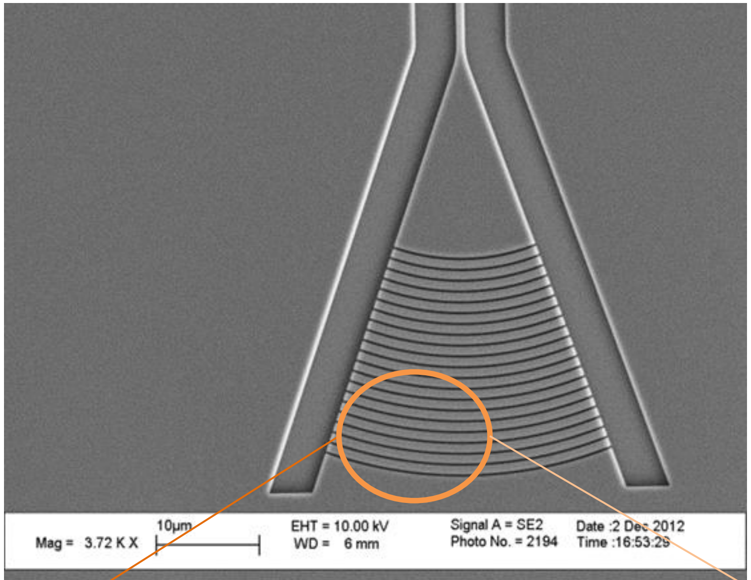

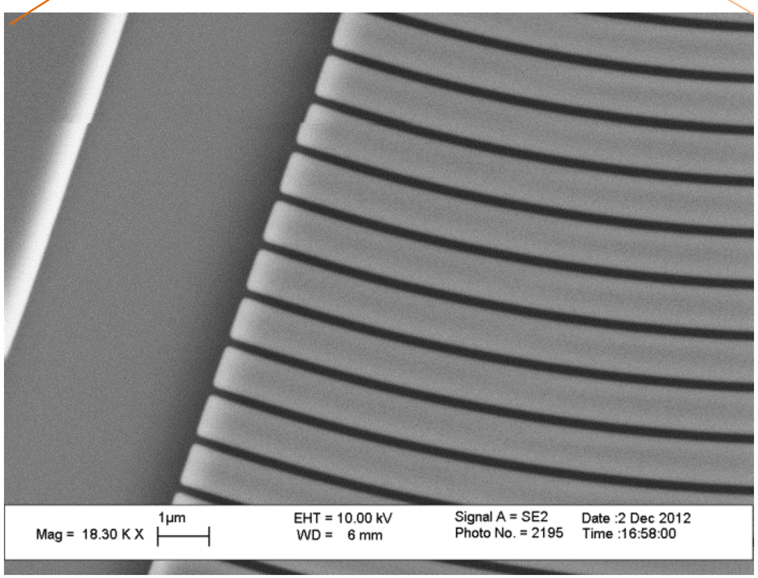

Image of a device prepared in Cadeance (Acrobat)

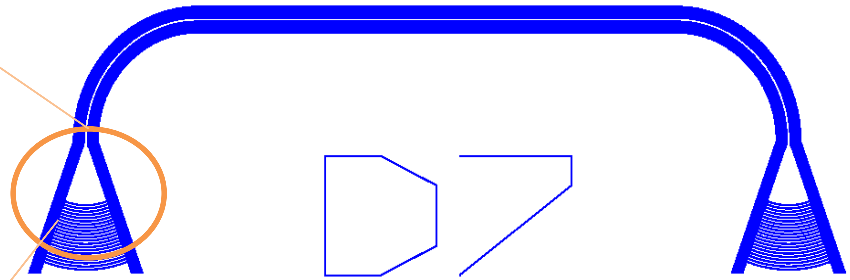

Parameters

d = 330nm, 450nm

ff = a/p (50-90%), height= h/d=0,5-1

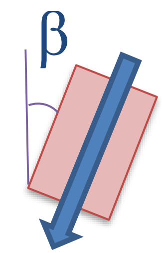

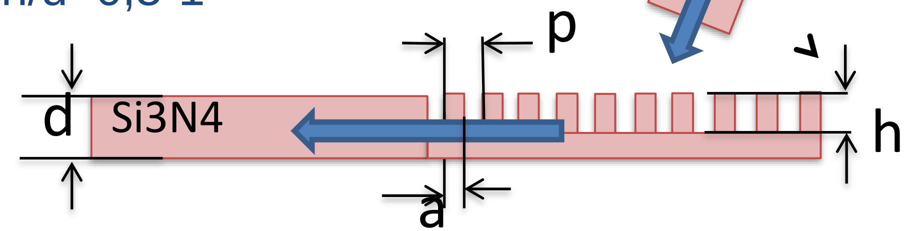

FF Variation

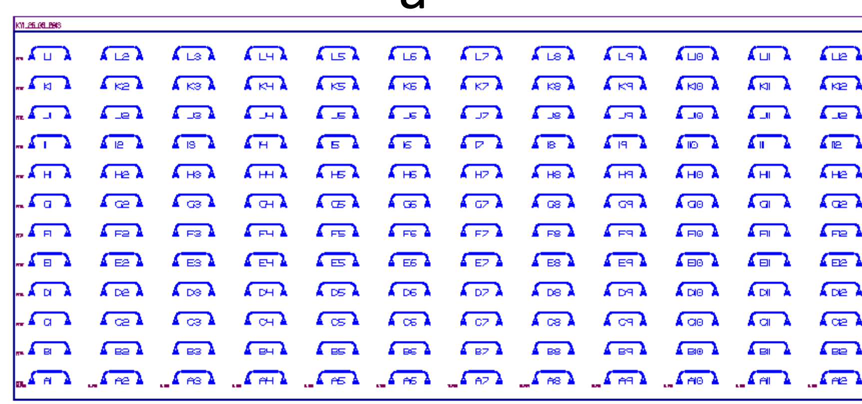

Variation of period FGC

On-chip detection efficiency (OCDE) vs nanowire width

SEM Image of a U-shaped nanowire

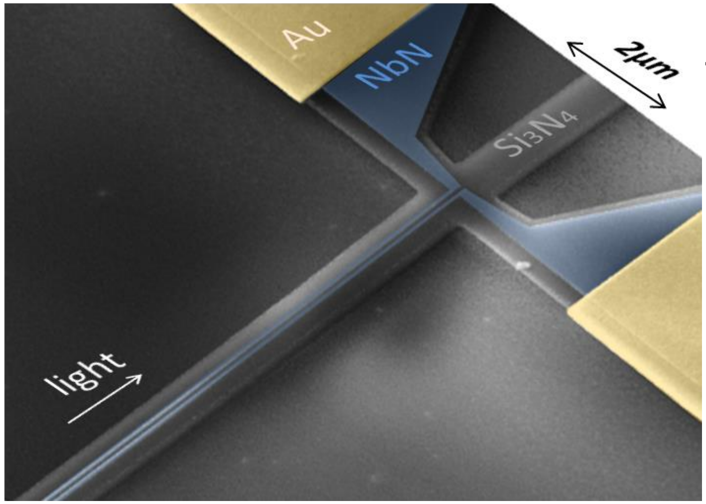

*OCDE=A*IQE*

OCDE vs NbN nanowire width (U-shaped)

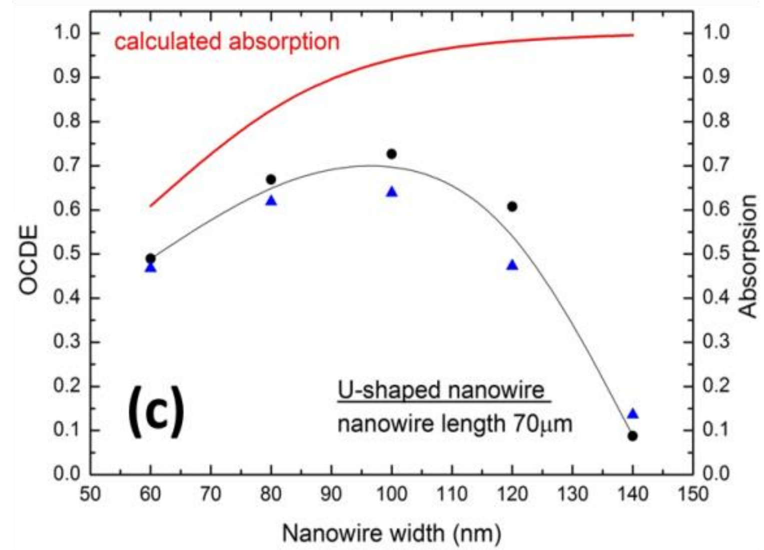

SEM Image of a W-shaped nanowire

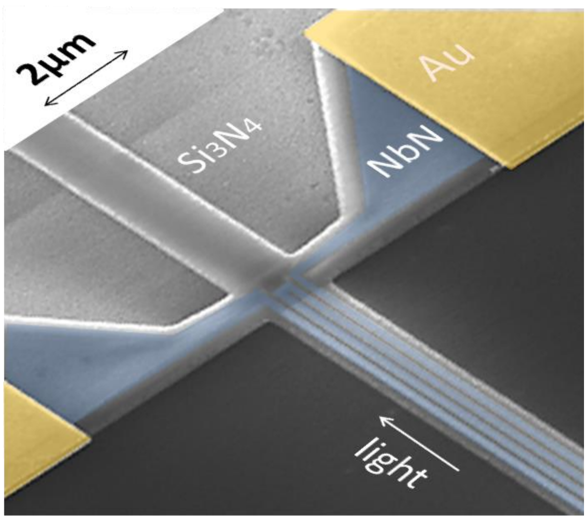

OCDE≈IQE

OCDE vs NbN nanowire width (W-shaped)

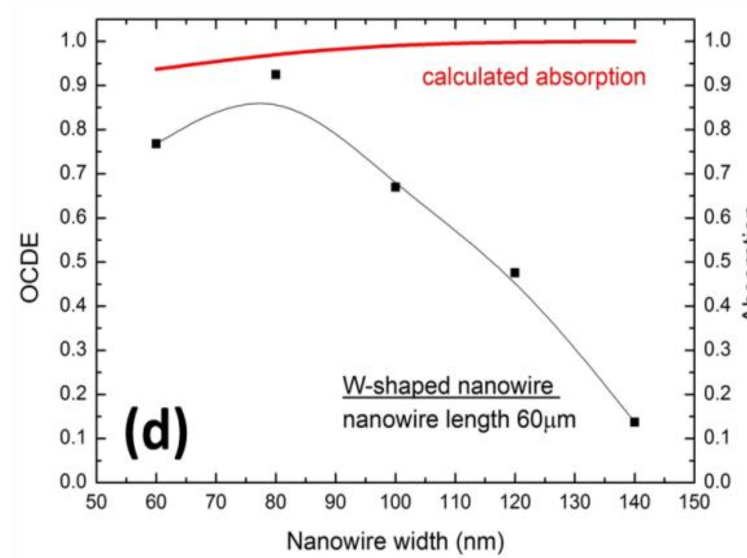

Waveguide-based SSPD characterization: detection efficiency, dark count rate and NEP vs bias

OCDE vs normalized bias current

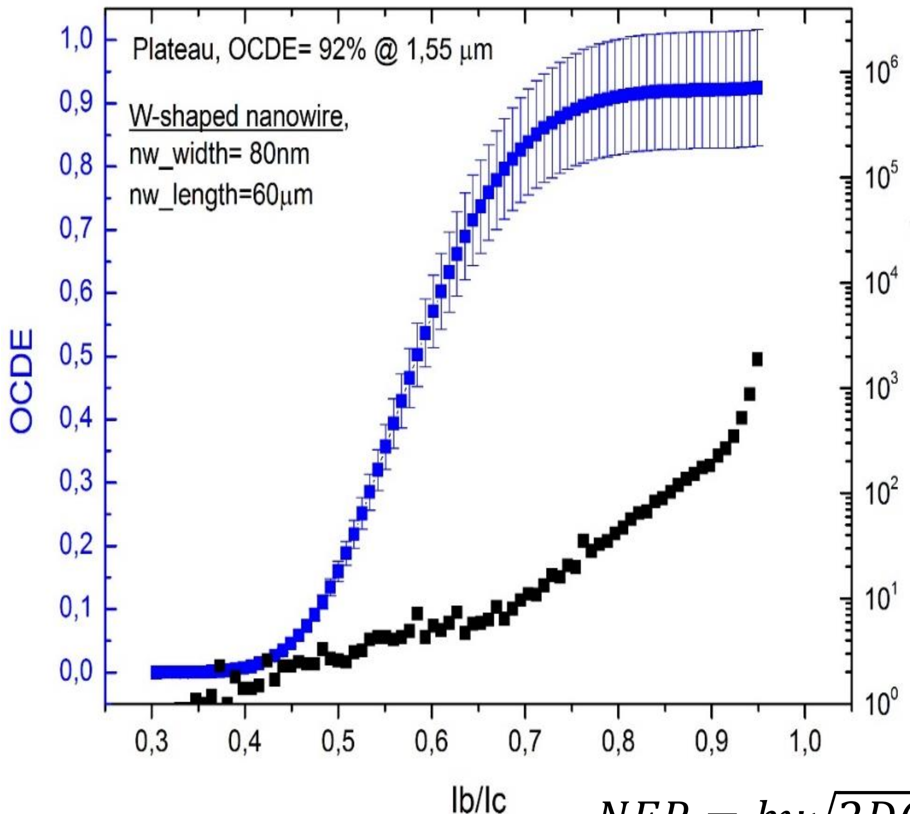

OCDE and NEP vs normalized bias current

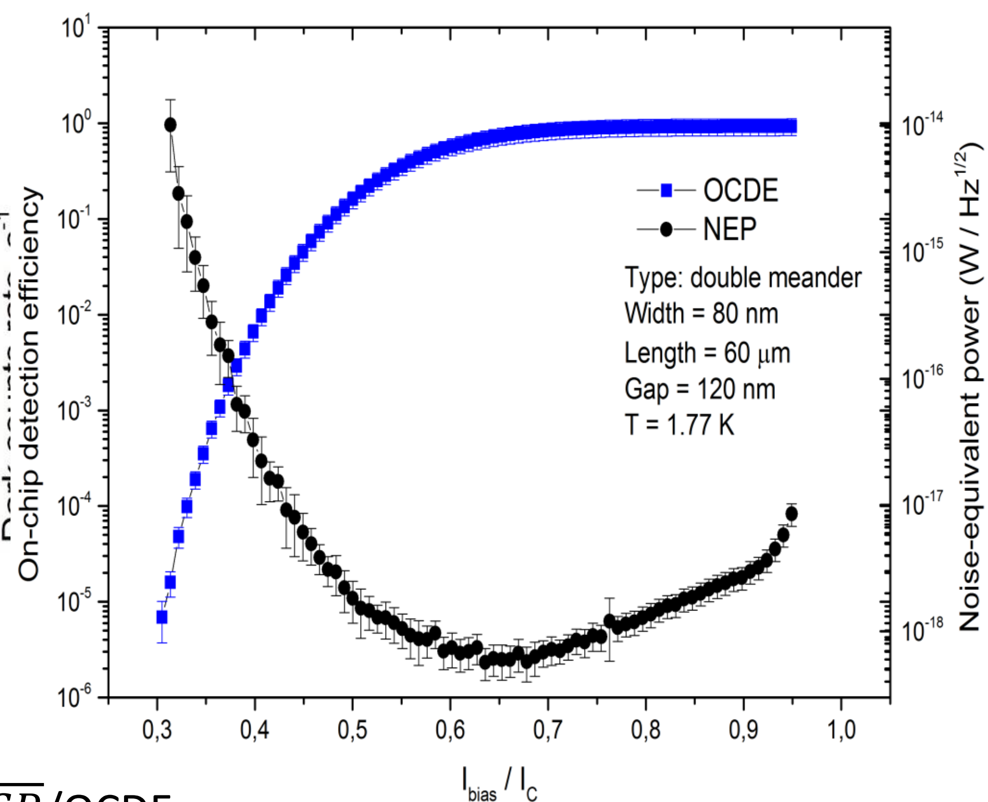

$$NEP = h\nu\sqrt{2DCR}/\text{OCDE}$$

O. Kahl, S. Ferrari, V. Kovalyuk, G. N. Goltsman, A. Korneev, and W. H. P. Pernice, “Waveguide integrated superconducting single-photon detectors with high internal quantum efficiency at telecom wavelengths.,” *Sci. Rep.*, vol. 5, no. February, p. 10941, 2015.

MZI with two directional couplers

Optical image of MZI with two directional couplers

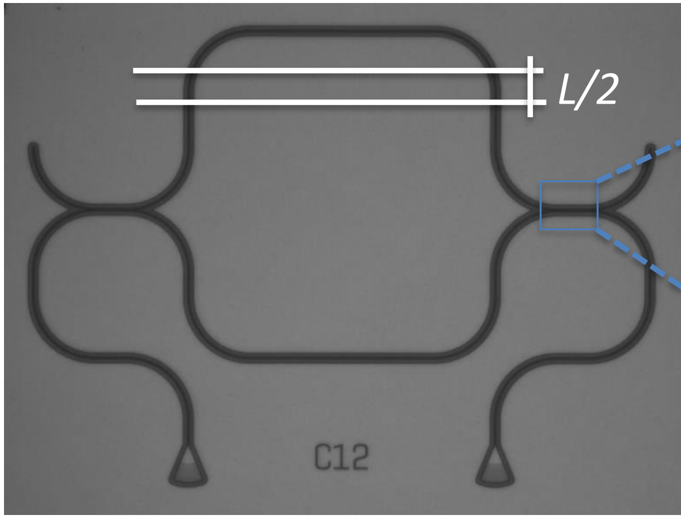

SEM image of the directional coupler

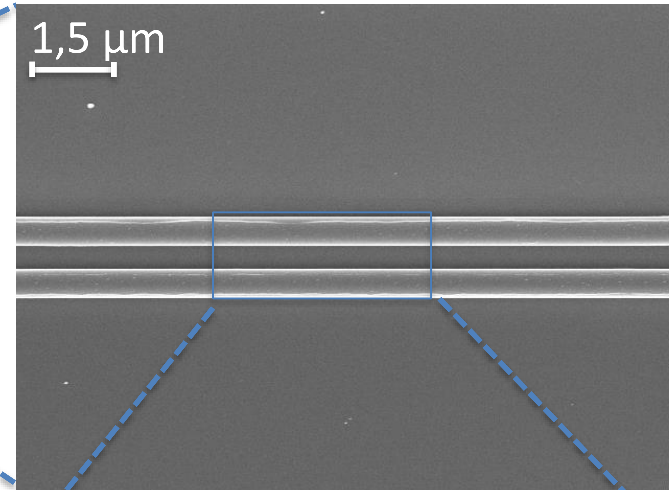

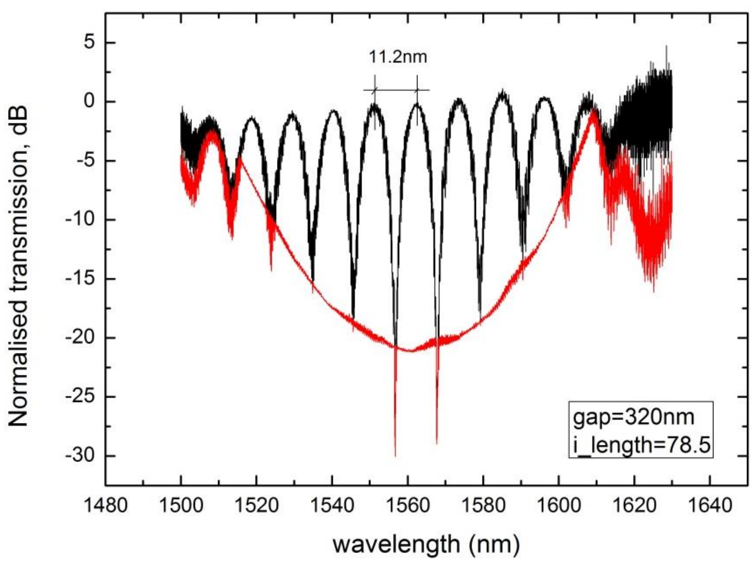

Normalized transmission MZI vs wavelength

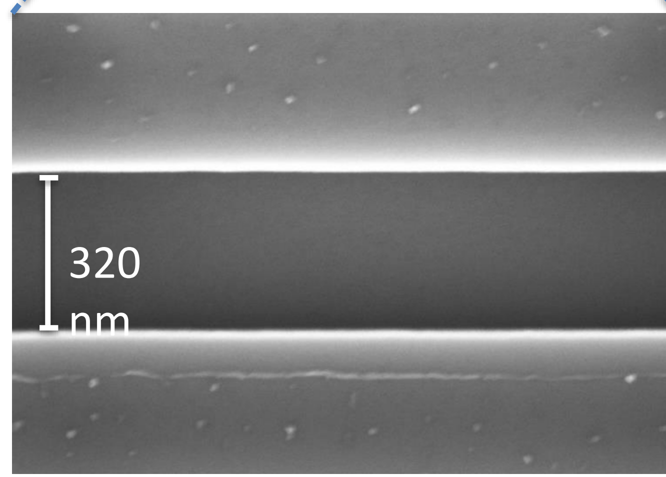

SEM image of the directional coupler (central part)

Fully integrated quantum photonic circuit with an electrically driven light source - waveguide-coupled semiconducting single-walled carbon nanotubes

Sc-SWCNT and two SNSPDs, all biased electrically

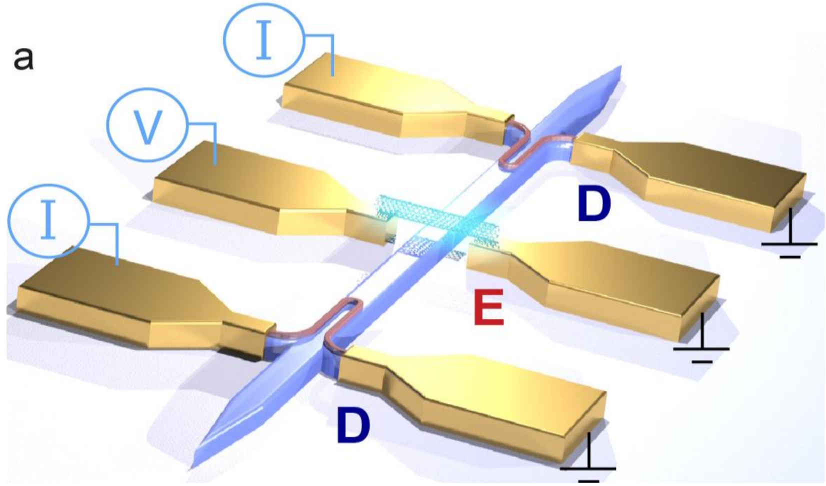

SSPD

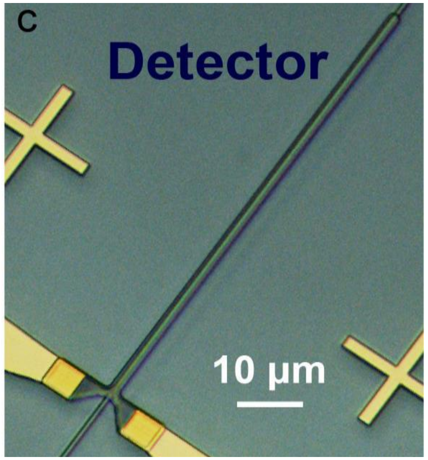

Optical micrograph

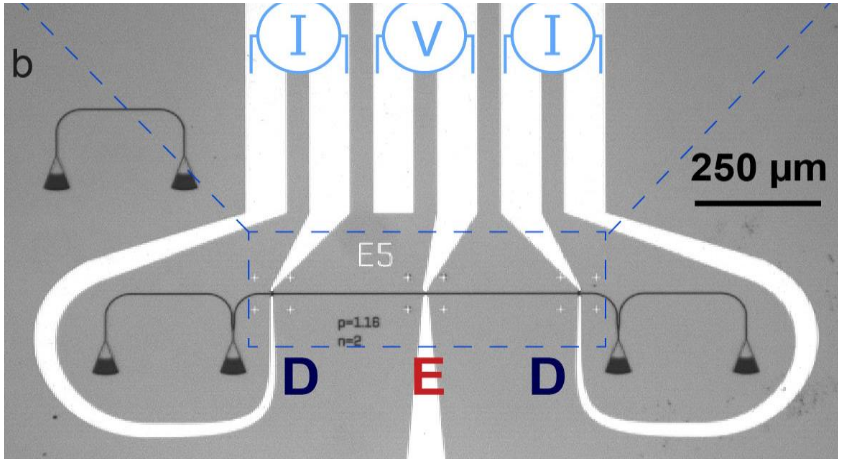

sc-SWCNT

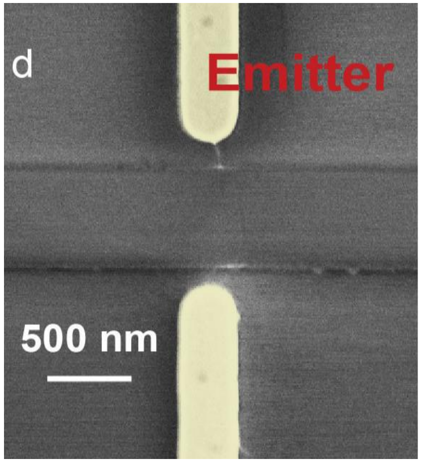

S. Khasminskaya, F. Pyatkov, K. Słowik, S. Ferrari, O. Kahl, V. Kovalyuk, P. Rath, A. Vetter, F. Hennrich, M. M. Kappes, G. Gol'tsman, A. Korneev, C. Rockstuhl, R. Krupke, and W. H. P. Pernice, "Fully integrated quantum photonic circuit with an electrically driven light source" *Nat. Photonics*, 10, 727–732 (2016)

Non-classical light from carbon nanotube

Coincidence histograms of non-classical light from sc-SWCNT

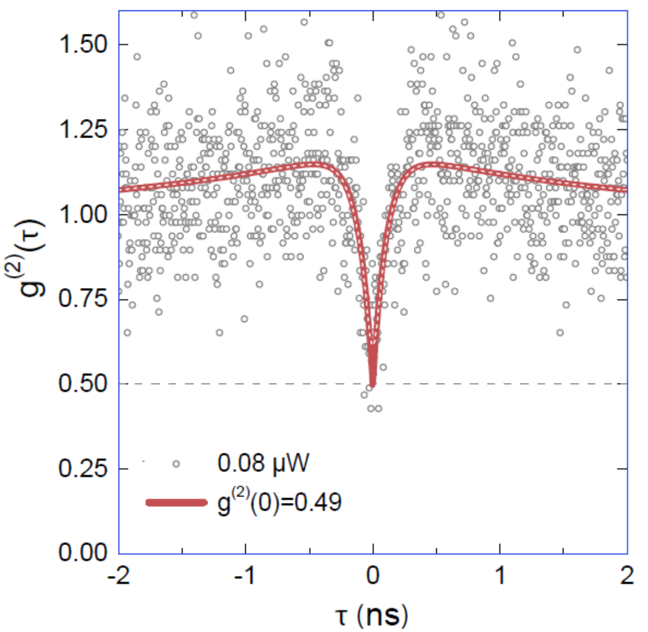

Correlation function at zero delay vs power

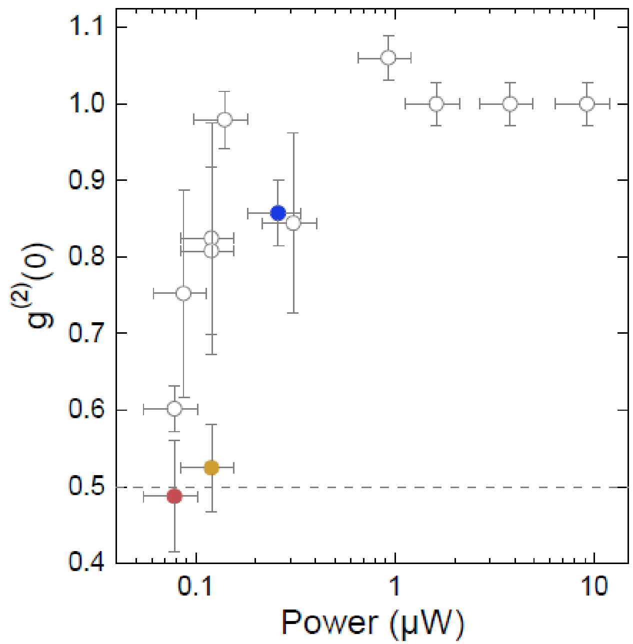

Antibunching (c_2) vs bunching amplitude (c_1)

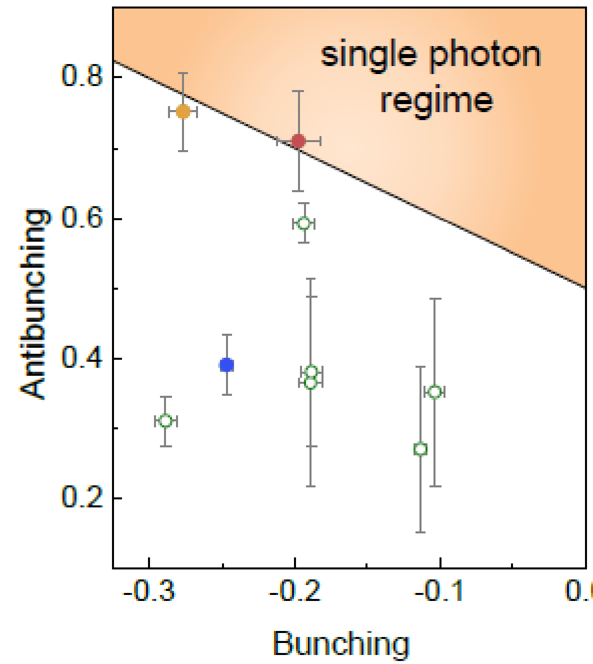

Fit equation: $g^{(2)}(\tau) = 1 - c_1 e^{-\gamma_1|\tau-\tau_0|} - c_2 e^{-\gamma_2|\tau-\tau_0|}$

Parameters: c_1, c_2 –amplitudes, γ_1, γ_2 - decay rates

S. Khasminskaya, F. Pyatkov, K. Słowik, S. Ferrari, O. Kahl, V. Kovalyuk, P. Rath, A. Vetter, F. Hennrich, M. M. Kappes, G. Gol'tsman, A. Korneev, C. Rockstuhl, R. Krupke, and W. H. P. Pernice, "Fully integrated quantum photonic circuit with an electrically driven light source" *Nat. Photonics*, 10, 727–732 (2016)

Spectrally resolved imaging with hybrid superconducting - nanophotonic circuits

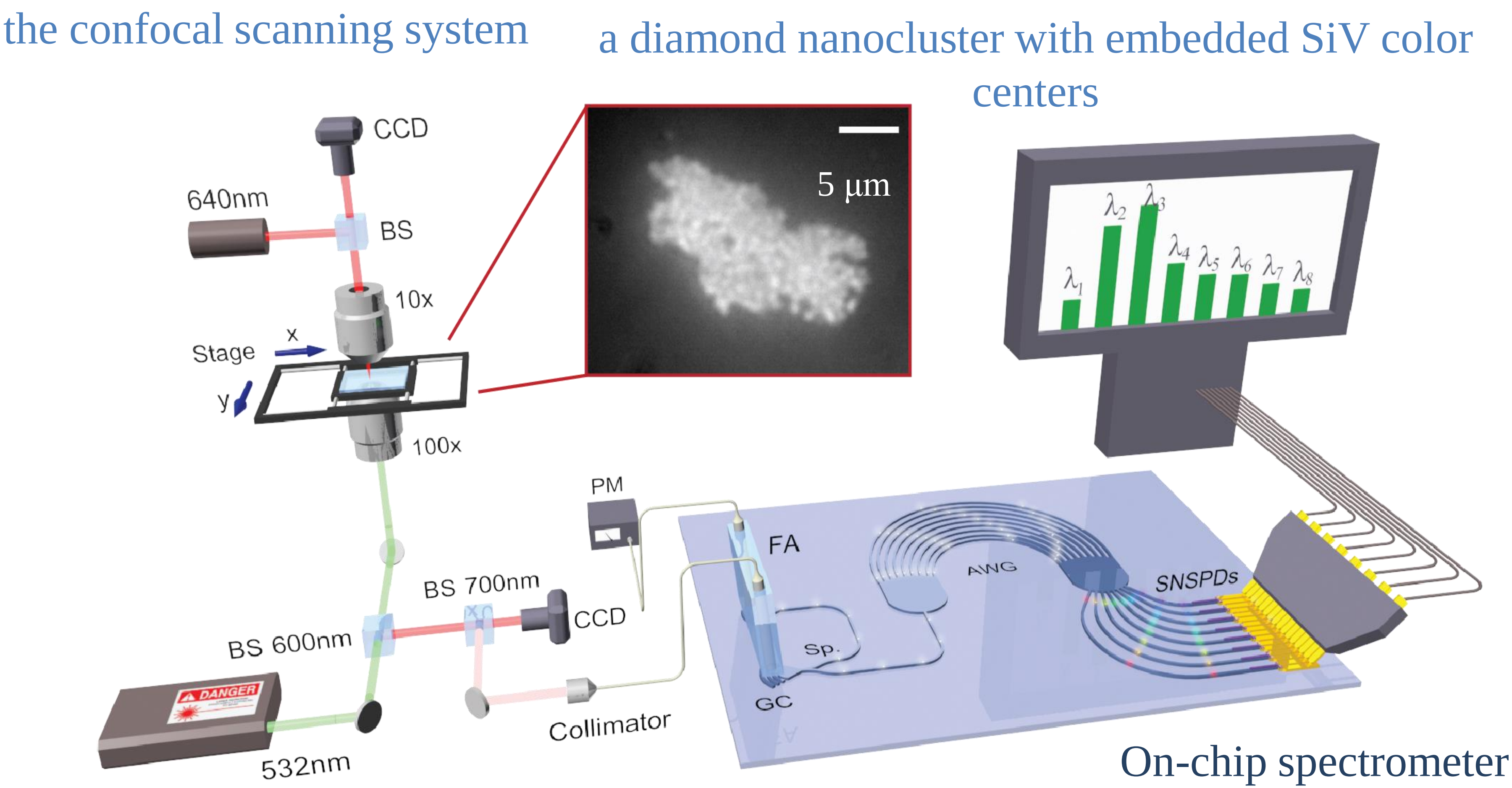

O. Kahl, S. Ferrari, V. Kovalyuk, A. Vetter, G. Lewes-Malandrakis, C. Nebel, A. Korneev, G. Goltsman, W. Pernice, Spectrally resolved single-photon imaging with hybrid superconducting - nanophotonic circuits, Optica, 2017.

On-chip spectrometer: arrayed waveguide grating and SSPDs

Arrayed waveguide grating

Single device

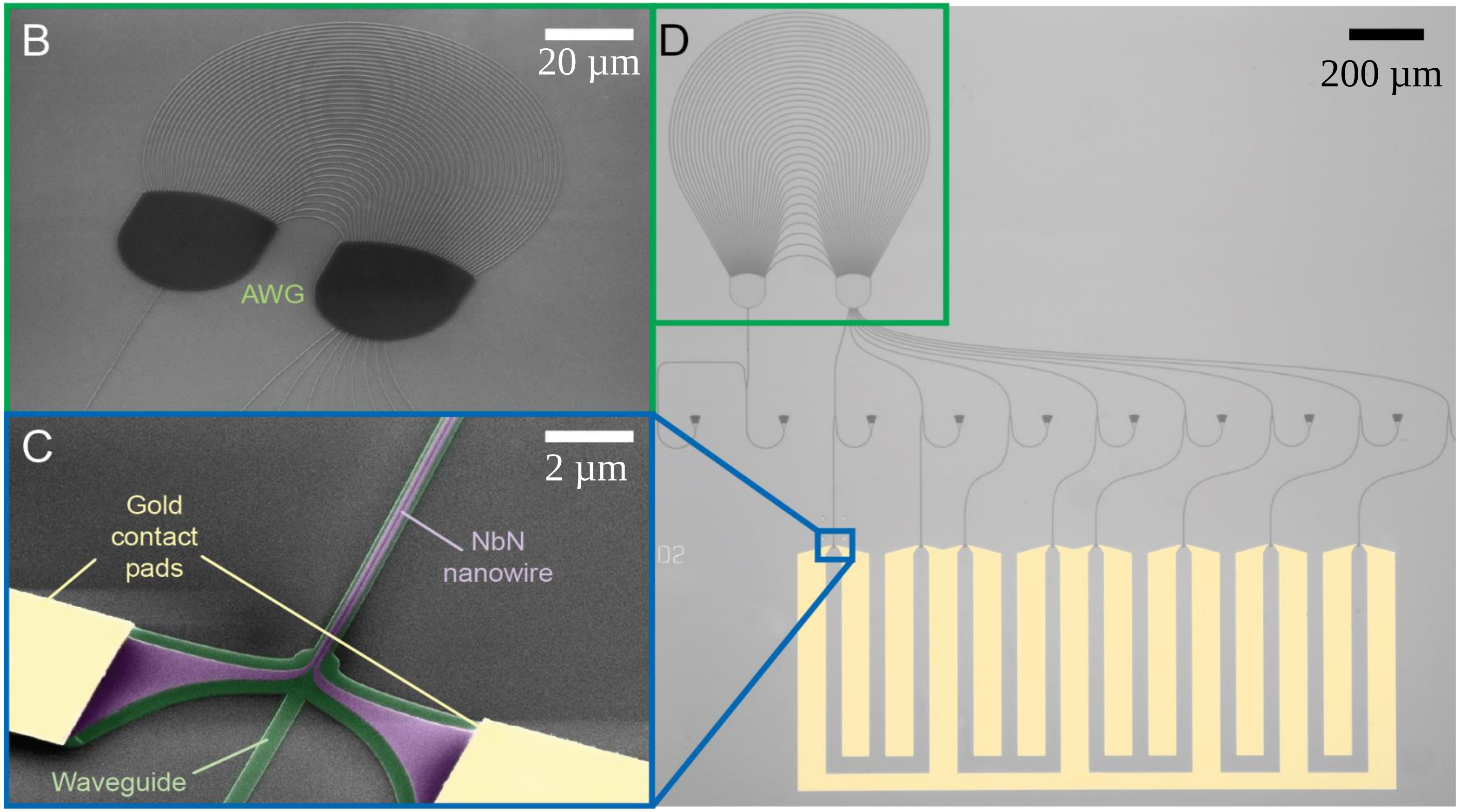

O. Kahl, S. Ferrari, V. Kovalyuk, A. Vetter, G. Lewes-Malandrakis, C. Nebel, A. Korneev, G. Goltsman, W. Pernice, Spectrally resolved single-photon imaging with hybrid superconducting - nanophotonic circuits, Optica, 2017..

Spatial map of the count rate from diamond nanocluster with embedded SiV color centers and decay time

Spatial map of the count rate

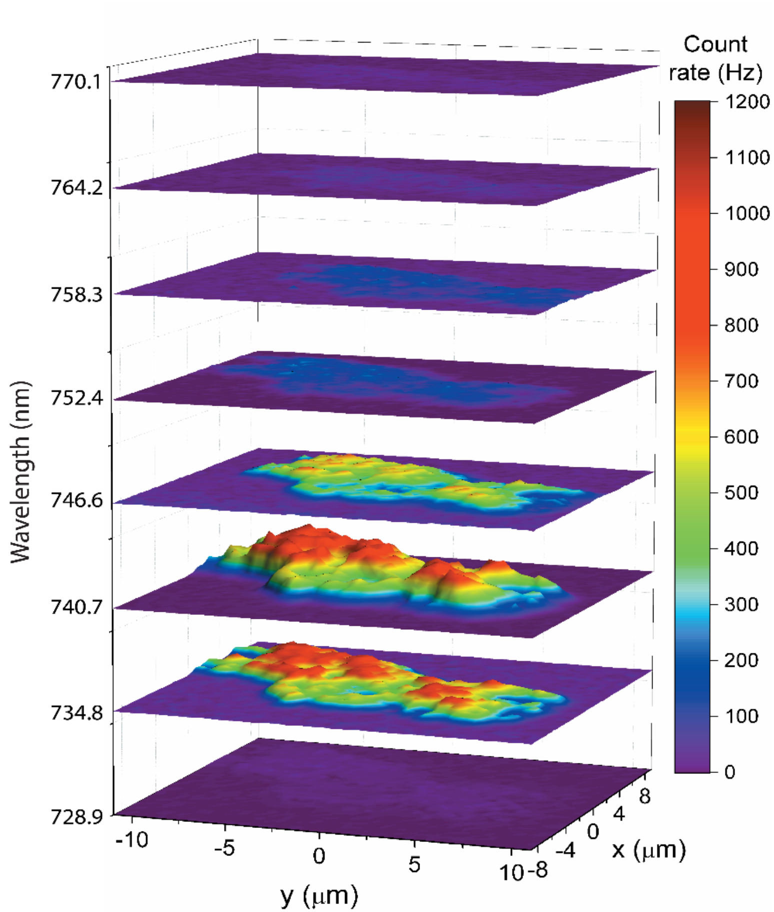

Decay time

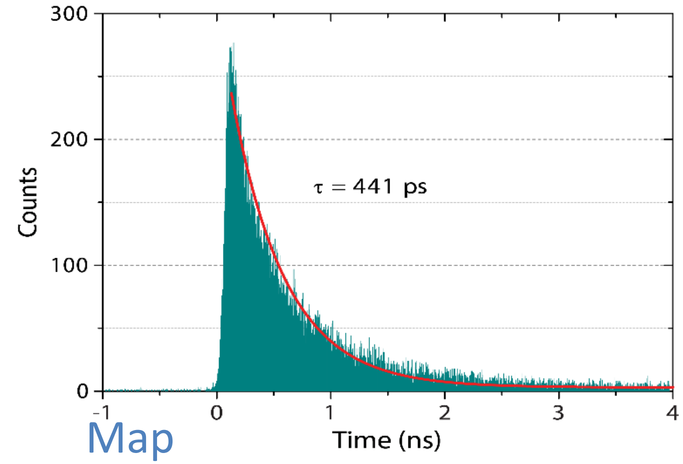

Map

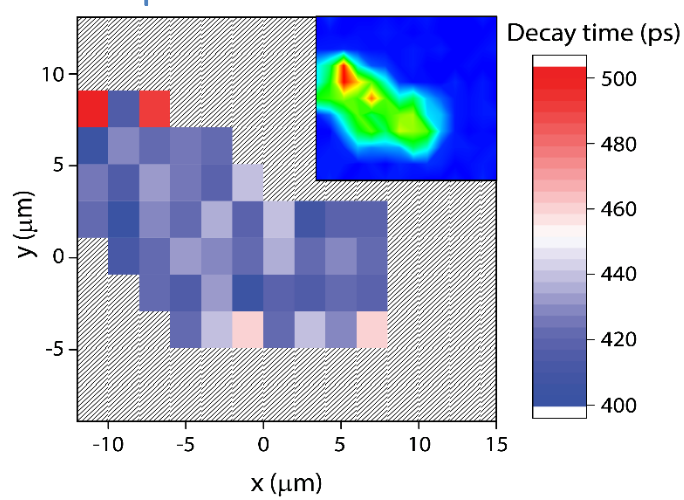

O. Kahl, S. Ferrari, V. Kovalyuk, A. Vetter, G. Lewes-Malandrakis, C. Nebel, A. Korneev, G. Goltsman, W. Pernice, Spectrally resolved single-photon imaging with hybrid superconducting - nanophotonic circuits, Optica, 2017.

Emission spectrum of silicon vacancy measured by on-chip spectrometer

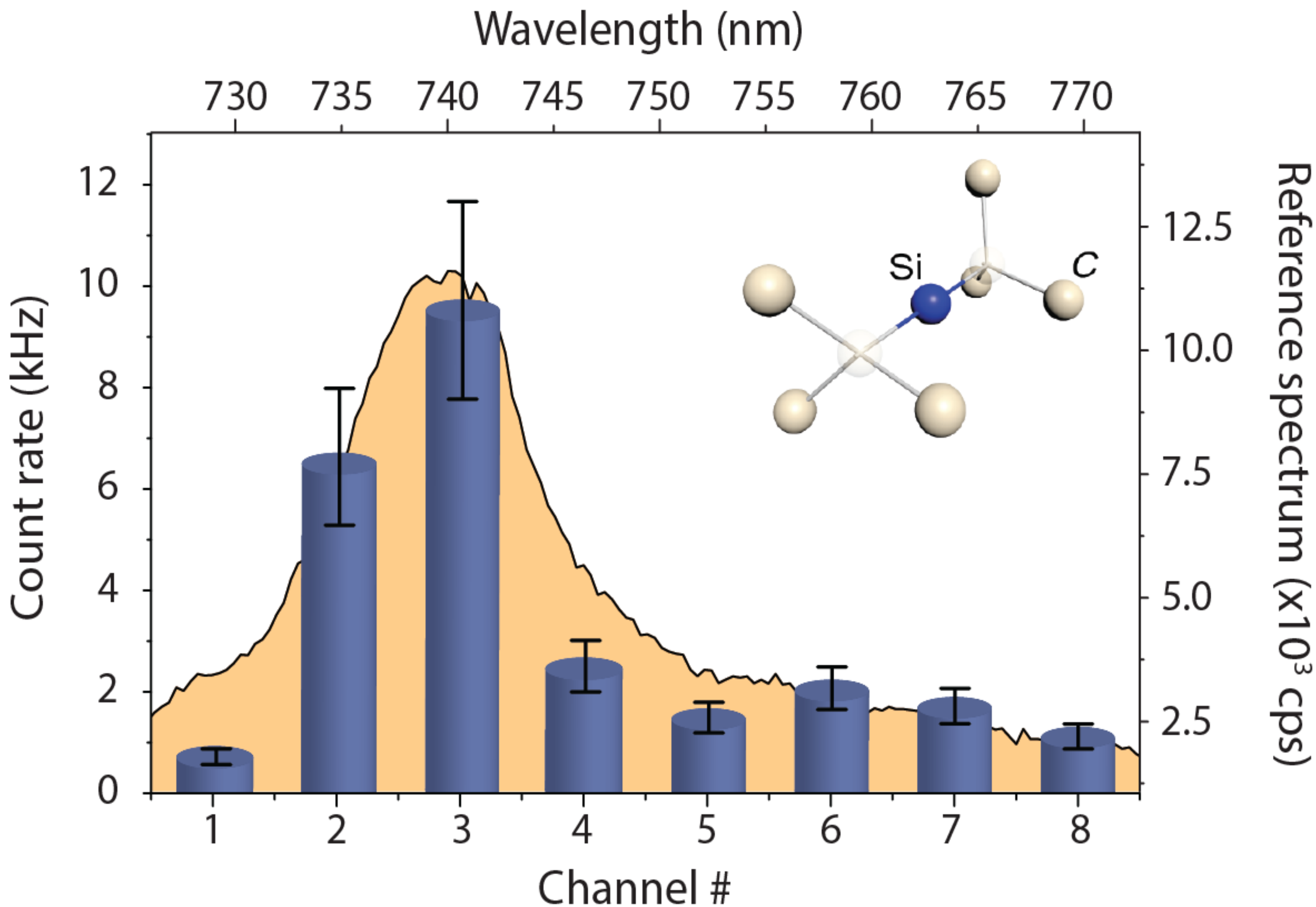

O. Kahl, S. Ferrari, V. Kovalyuk, A. Vetter, G. Lewes-Malandrakis, C. Nebel, A. Korneev, G. Goltsman, W. Pernice, Spectrally resolved single-photon imaging with hybrid superconducting - nanophotonic circuits, Optica, 2017..

SSPD as a photon counting mixer: Measurement setup and operation principle

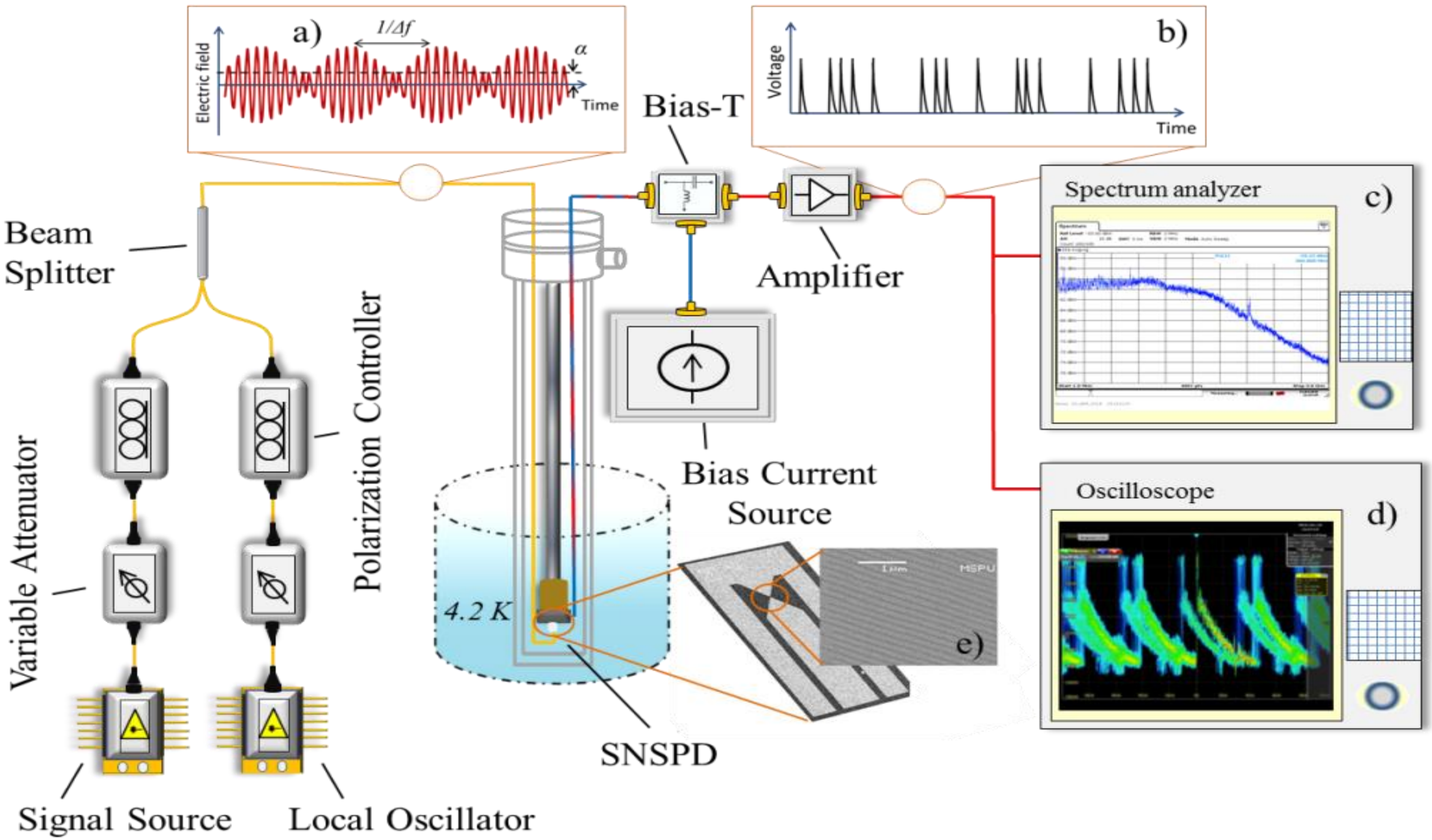

M. Shcherbatenko, Y. Lobanov, A. Semenov, V. Kovalyuk, A. Korneev, R. Ozhegov, A. Kazakov, B. M. Voronov, and G. N. Goltsman, "Potential of a superconducting photon counter for heterodyne detection at the telecommunication wavelength," Opt. Express 24, 30474-30484 (2016)

Amplified pulses from SSPD

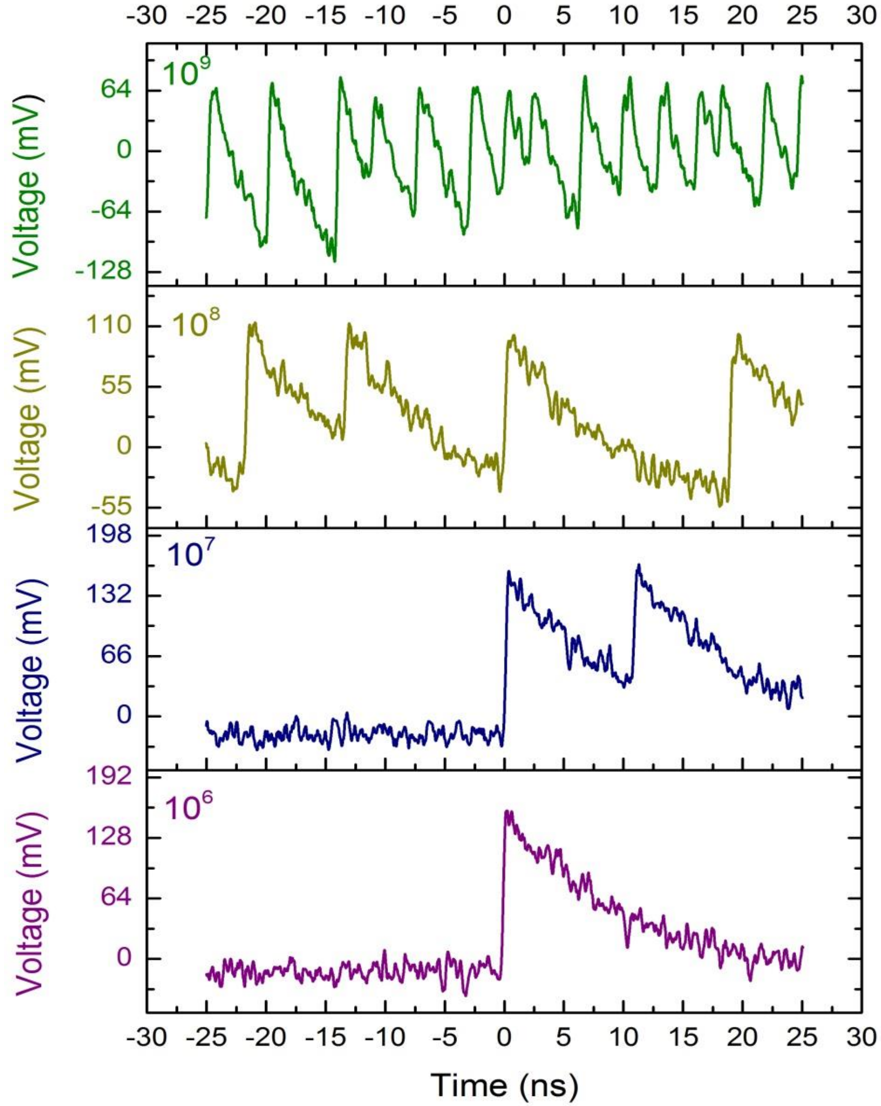

$\Phi_{LO}= 10^9(ph/s)$

$\Phi_{LO}= 10^8(ph/s)$

$\Phi_{LO}= 10^7(ph/s)$

$\Phi_{LO}= 10^6(ph/s)$

Waveguide-based setup with highly coherent laser as LO and acousto-optical modulator

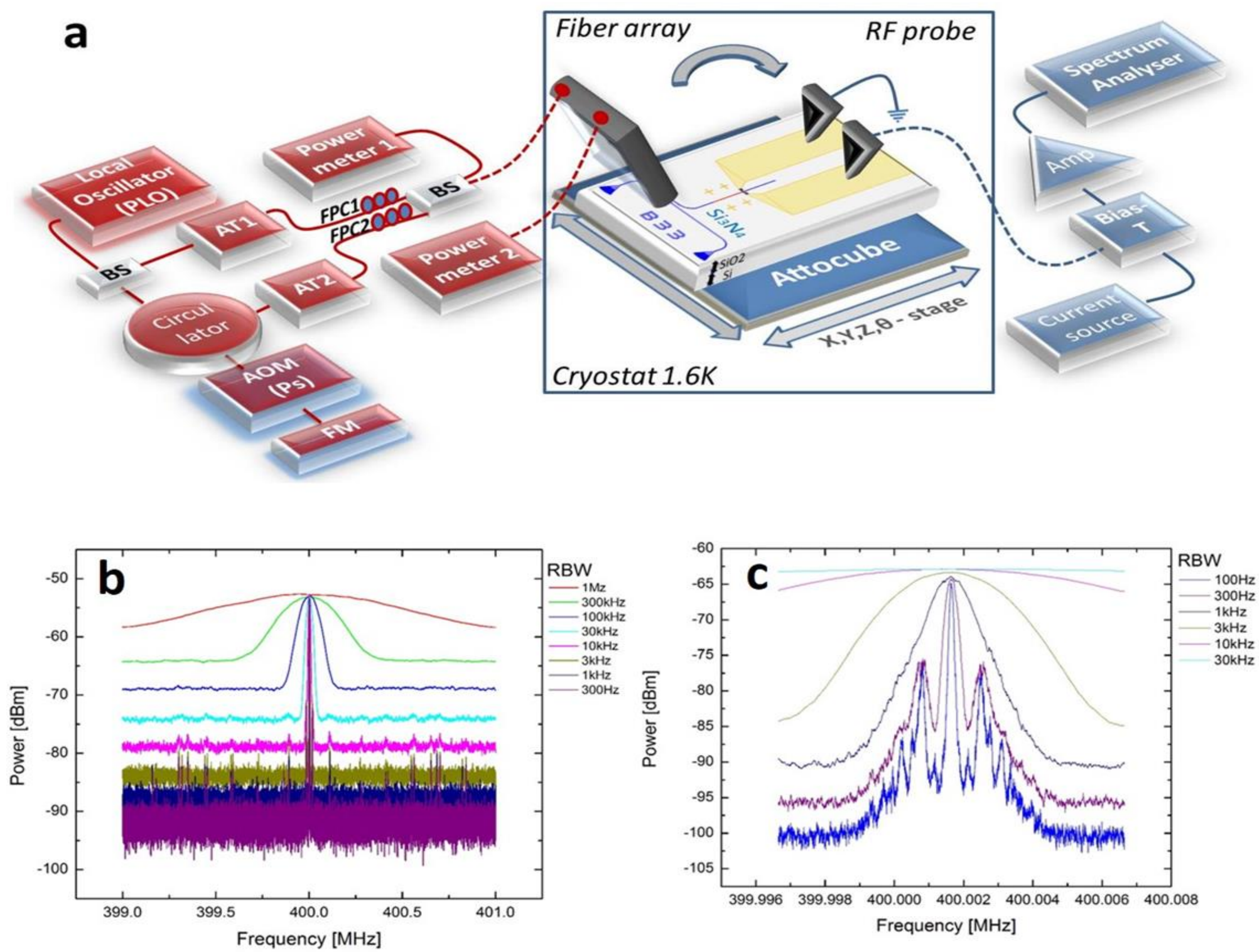

V. Kovalyuk, S. Ferrari, O. Kahl, A. Semenov, M. Shcherbatenko, Y. Lobanov, R. Ozhegov, A. Korneev, N. Kaurova, B. Voronov, W. Pernice, and G. Gol’tsman, “On-chip coherent detection with quantum limited sensitivity,” Sci. Rep., vol. 7, no. 4812, 2017.

Waveguide-based SSPD: power at IF versus bias and photon flux of a signal laser

Power at IF versus bias current for different photon flux from signal laser

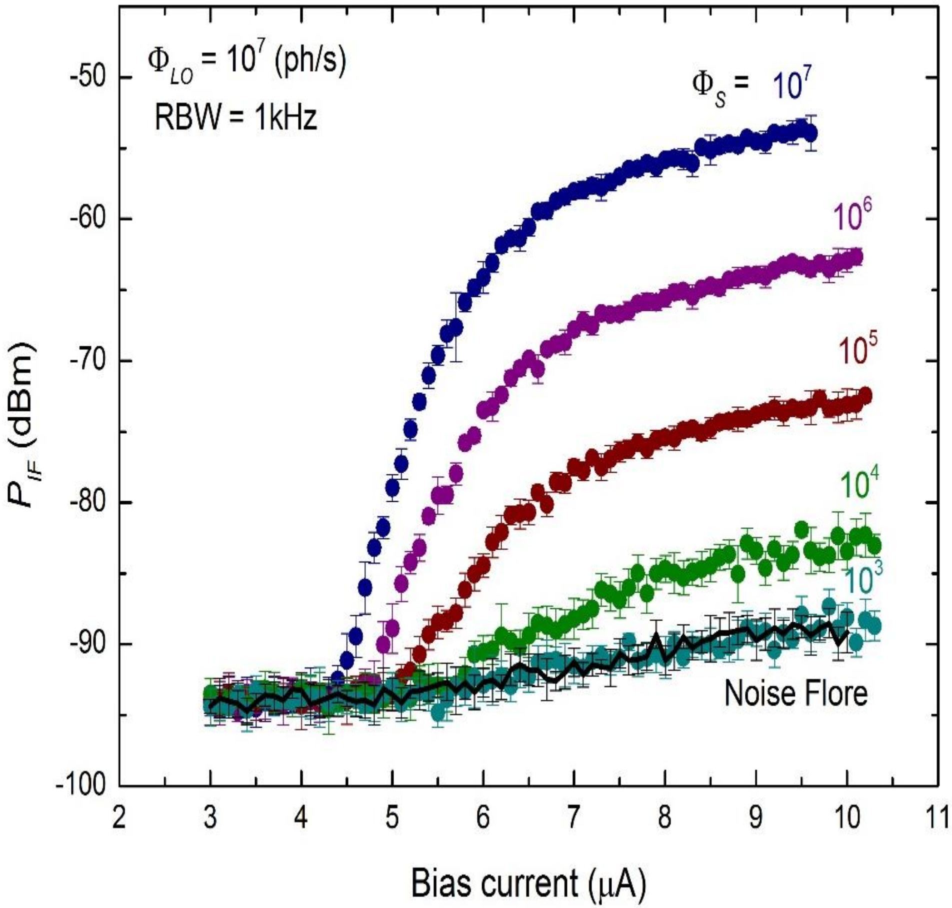

Power at IF versus photon flux of a signal laser for different photon flux from local oscillator

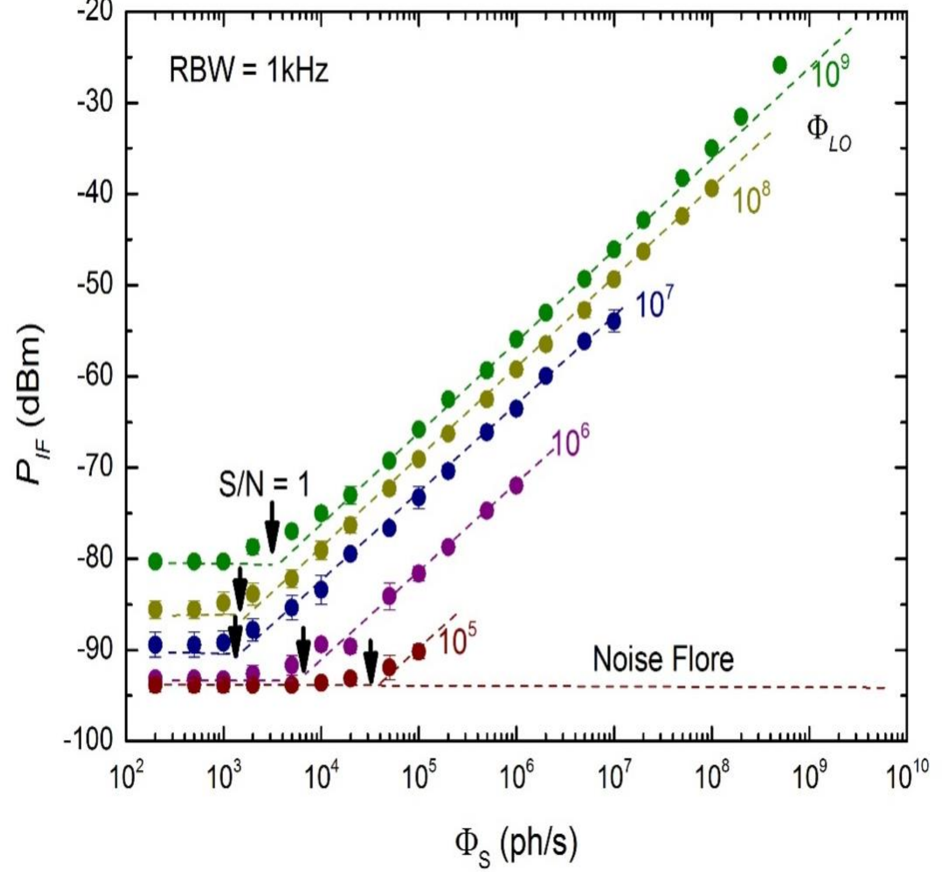

V. Kovalyuk, S. Ferrari, O. Kahl, A. Semenov, M. Shcherbatenko, Y. Lobanov, R. Ozhegov, A. Korneev, N. Kaurova, B. Voronov, W. Pernice, and G. Gol’tsman, “On-chip coherent detection with quantum limited sensitivity,” Sci. Rep., vol. 7, no. 4812, 2017.

Time-Domain Technique based on recording time moments of counts and digital post-processing

Short fragment of sequence of recorded counts

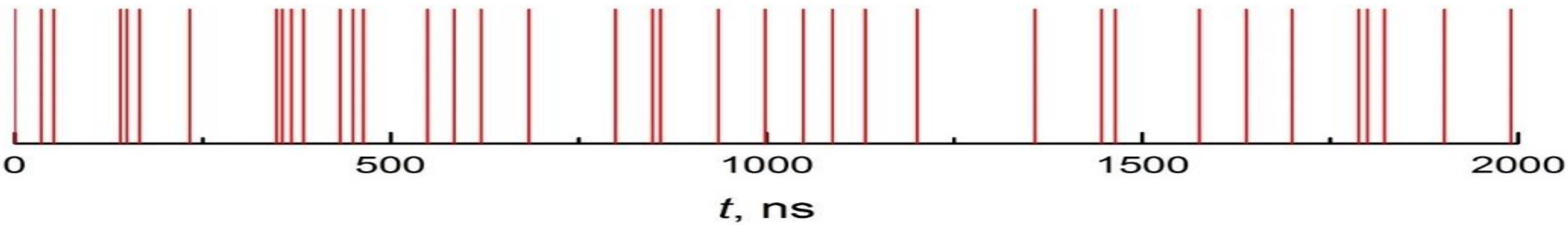

Second-order correlation function, solid curve – fit by dumped oscillations

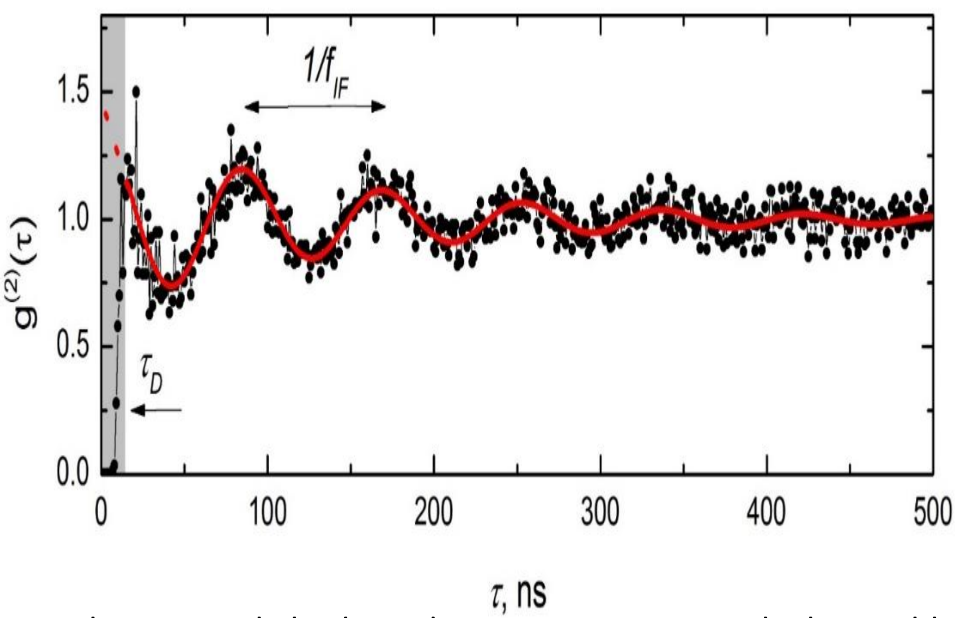

Fourier-spectrum; dashed line – linear fit for statistical noise background

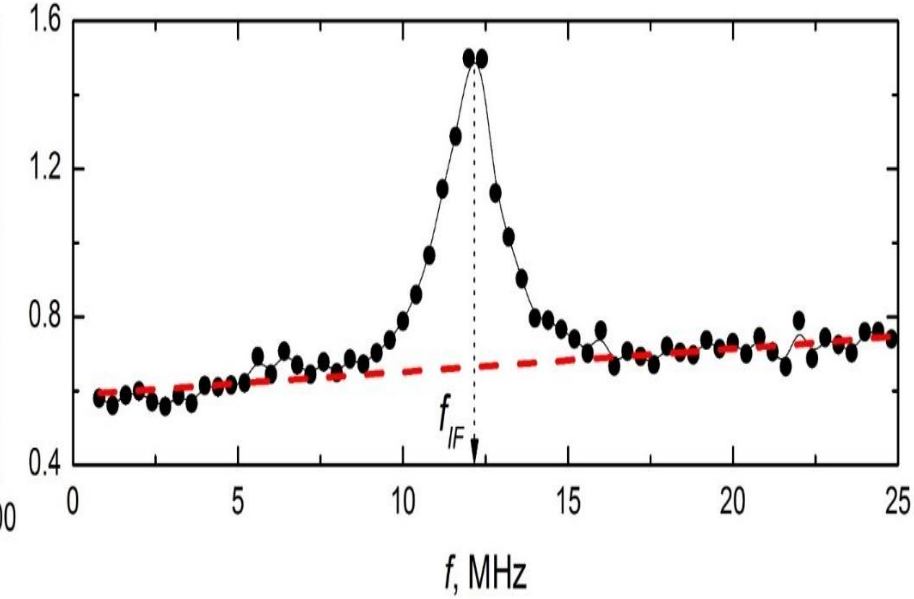

Y Lobanov, M Shcherbatenko, A Semenov, VKovalyuk, O Kahl, S Ferrari, A Korneev, R Ozhegov, N Kaurova, B Voronov, W H P Pernice and G Gol'tsman, "Superconducting Nanowire Single hoton Detectorfor Coherent Detection of Weak Signals" IEEE Transactions on Applied Superconductivity, 27, (4) (2017)

With statistical analysis of the time domain data we see that we are still far from limitation by dark count background and that the LO power can be decreased by many orders of magnitude, down to the atto-watt range

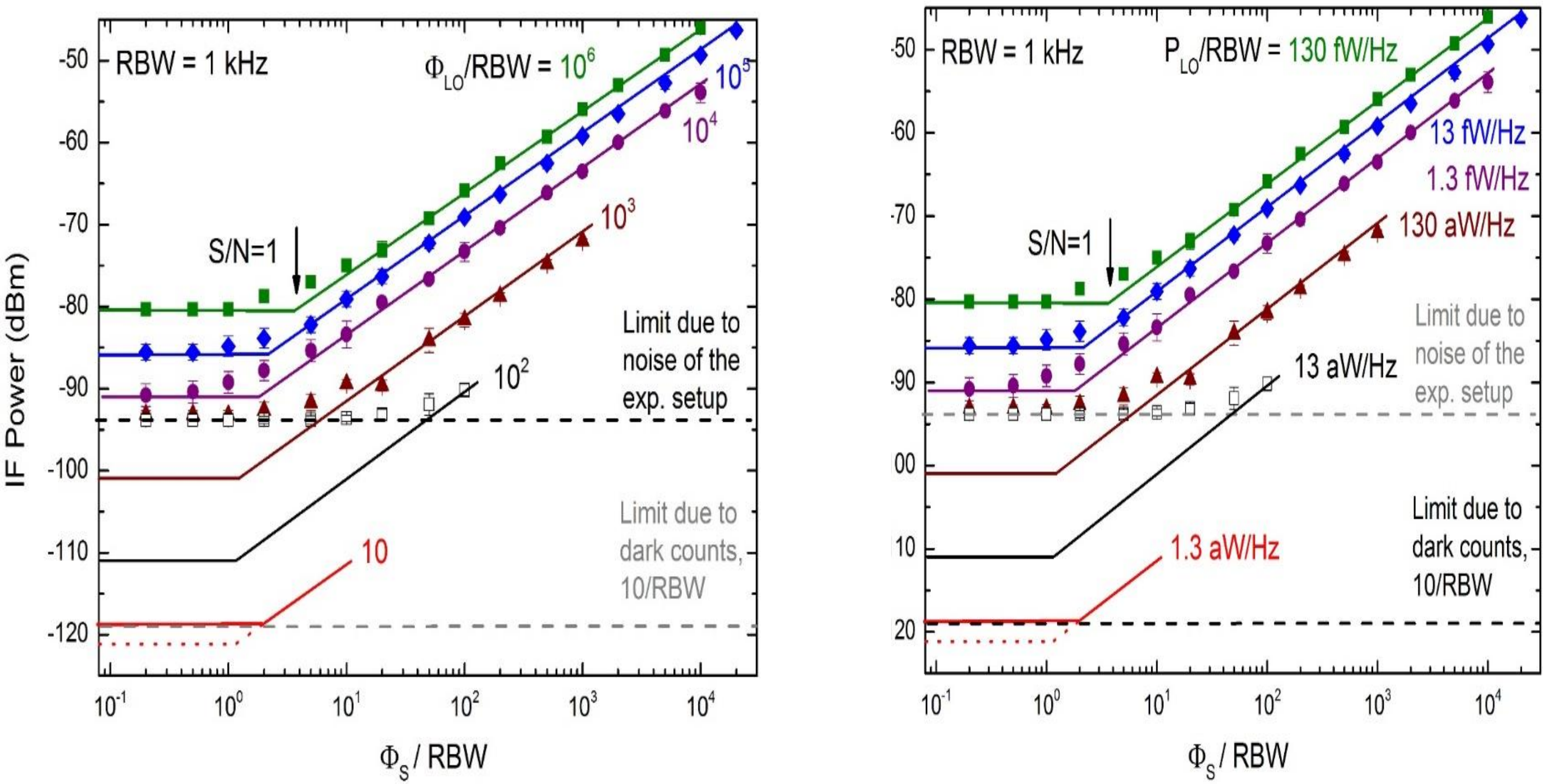

Y Lobanov, M Shcherbatenko, A Semenov, VKovalyuk, O Kahl, S Ferrari, A Korneev, R Ozhegov, N Kaurova, B Voronov, W H P Pernice and G Gol’tsman, “Superconducting Nanowire Single hoton Detectorfor Coherent Detection of Weak Signals” IEEE Transactions on Applied Superconductivity, 27, (4) (2017)

Conclusions

- Travelling wave SSPDs - superconducting stripes on optical waveguide demonstrate near-unity On-Chip Detection Efficiency and very good scalability.
- Promising single-photon platform for Quantum-Photonic Integrated Circuits (QPICs) based on Silicon Nitride on Si technology and combined on-chip: single photon sources - electrically driven waveguide-coupled semiconducting single-walled carbon nanotubes, linear optical elements like grating couplers, beam splitters, MZ interferometers and SSPDs as single-photon detectors.
- Heterodyne receiver based on SSPD mixer requires optimal local oscillator power that can be decreased by many orders of magnitude, down to the atto-watt range. This is promising for on-chip large heterodyne arrays.
- The realization of large scale QPICs can produce a profound impact on science and technology, material engineering, as well as quantum information processing including quantum computing, simulation and metrology.

Thank you for your attention!

S. Bogdanov, M.Y. Shalaginov, A. Boltasseva, V.M. Shalaev, Opt. Mater. Express, 7, 111-132 (2017) "Material platforms for integrated quantum photonics"

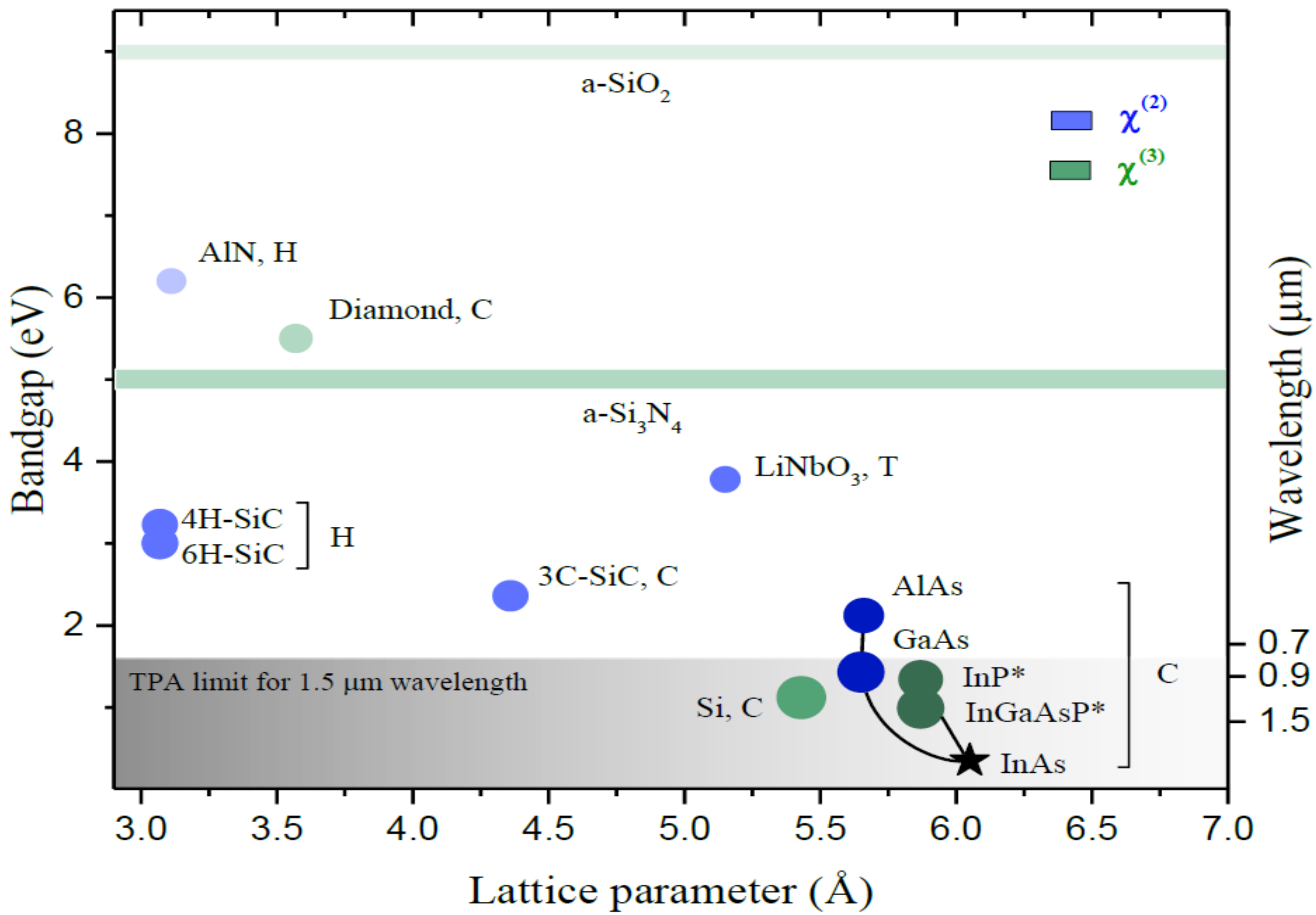

Properties of optical materials used in QPICs. Crystalline materials are represented by circles, while amorphous materials, (SiO2 and Si3N4) are shown with stripes, since they do not possess a lattice constant. The circle diameters (and stripe thicknesses) are proportional to the refractive indices. Blue and green colors indicate second- and third-order nonlinearities respectively. The color shades qualitatively describe the strengths of nonlinear optical responses. Darker shades correspond to higher values of nonlinear coefficients. InAs is used in quantum dots and is indicated with a star. Crystal structure abbreviations: C – cubic, H – hexagonal, T – trigonal.

M. Kues, C. Reimer, P. Roztocki, L.R. Cortés, S. Sciara, B. Wetzel, Y. Zhang, A. Cino, S.T. Chu, B.E. Little, D.J. Moss, L. Caspani, J. Azaña, R. Morandotti, Nature, **546**, 622-626 (2017) "On-chip generation of high-dimensional entangled quantum states and their coherent control"

Experimental setup for high-dimensional quantum state generation and control.

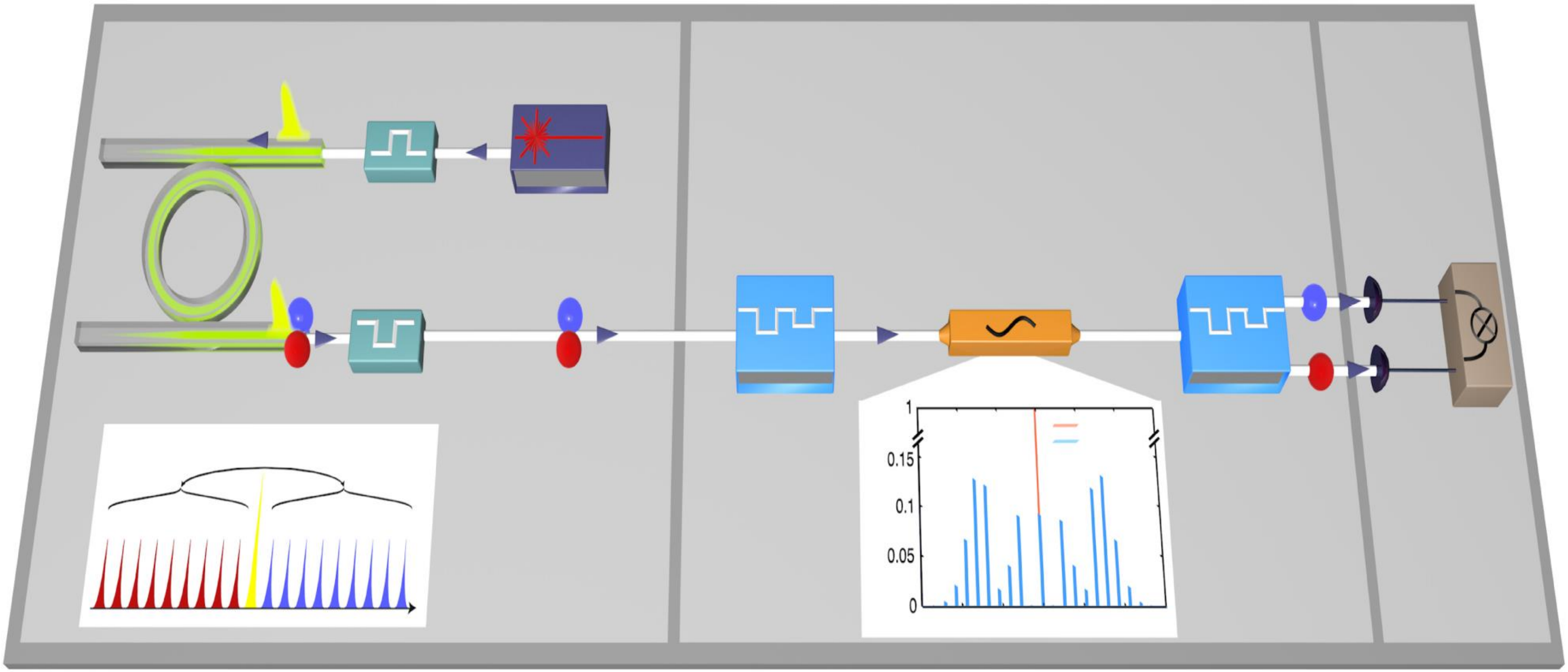

A passively mode-locked laser was coupled into the integrated micro-ring resonator after being spectrally filtered to excite precisely a single resonance. Spontaneous four-wave mixing (SFWM) (see left inset) led to the generation of photon pairs (signal and idler) spectrally symmetric to the excitation and in a quantum superposition of the frequency modes defined by the resonances. Programmable filters and a modulator were used for manipulating the state (the right inset shows frequency sideband generation by the modulator as a function of frequency ν), before the signal and idler photons were detected by two single photon counters.

M. Kues, C. Reimer, P. Roztocki, L.R. Cortés, S. Sciara, B. Wetzel, Y. Zhang, A. Cino, S.T. Chu, B.E. Little, D.J. Moss, L. Caspani, J. Azaña, R. Morandotti, Nature, **546**, 622-626 (2017) "On-chip generation of high-dimensional entangled quantum states and their coherent control"

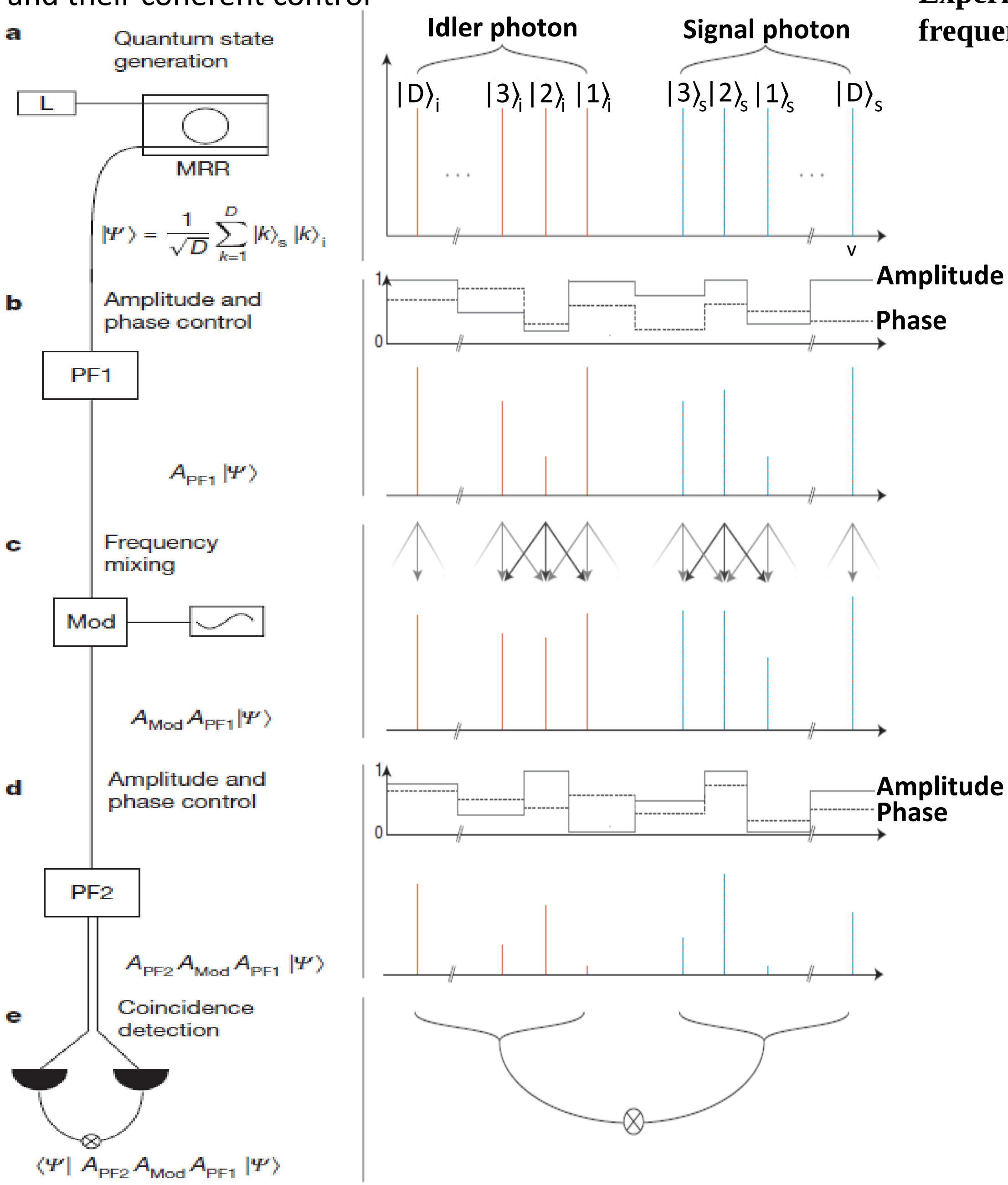

Experimental implementation of the coherent control of frequency-entangled high-dimensional quantum states.

Individual steps to control, manipulate and characterize the high-dimensional quantum states are displayed, showing for each one the equipment used and a schematic of the modification imposed on the quantum state in the spectral domain. a, The initial states $|\Psi\rangle$ were generated using the microring resonator (MRR)-based operational principle illustrated in Fig. 1. b, Using a programmable filter (PF1), any arbitrary spectral phase and amplitude mask can be imposed on the quantum states for manipulation. c, An electro-optic modulator (Mod) driven by a radio-frequency synthesizer was used to coherently mix different frequency components of the high-dimensional states. In particular, such an operation can be precisely controlled by using appropriate electronic radio-frequency signals for the mixing of 2, 3, 4 or (in principle) more adjacent frequency modes. d, A second programmable filter (PF2) can impose an amplitude and phase mask and route the signal and idler to two different paths. e, The photons were then detected using single photon counters and timing electronics. This step, together with the previous adjustable coherent control, allows the implementation of adaptable projections, which can then be used, for example, for Bell measurements or quantum state tomography. The complete mathematical description of all operations (indicated by APF1, APF2 and AMod) can be found in Methods.

S. Bogdanov, M.Y. Shalaginov, A. Boltasseva, V.M. Shalaev, Opt. Mater. Express, 7, 111-132 (2017)
"Material platforms for integrated quantum photonics"

Lithium niobate and silicon carbite platforms

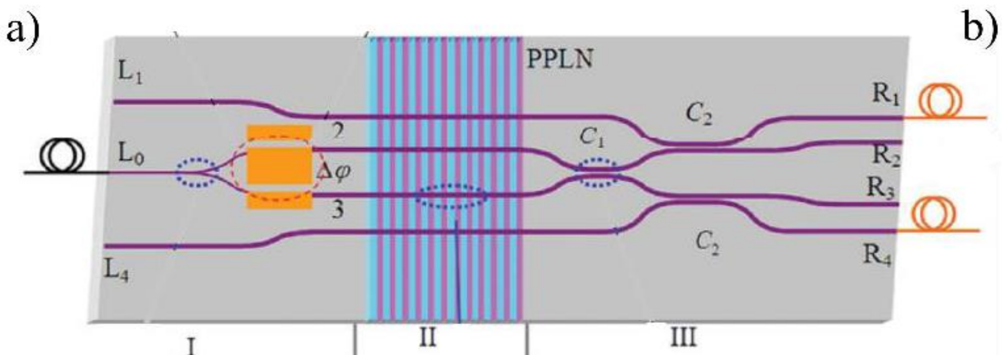

(a) A lithium niobate chip with nonlinear, passive and active elements, allowing generation and characterization of entangled photon pairs [110].

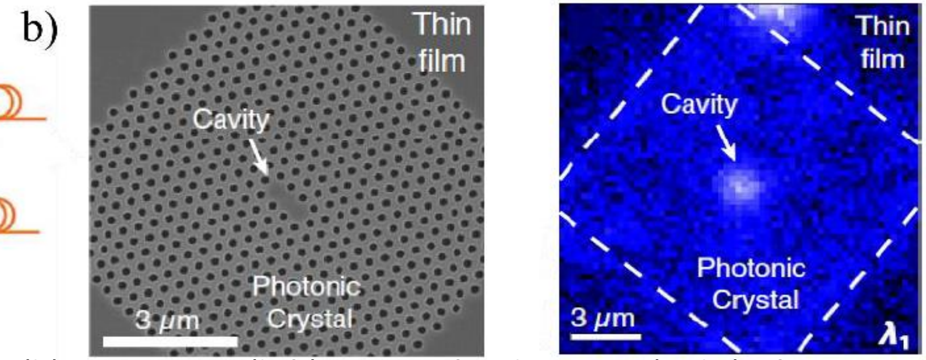

(b) SEM image (left) and confocal PL scan (right) of a SiC-on-Si photonic crystal cavity containing an ensemble of Ky5 spin defects [124].

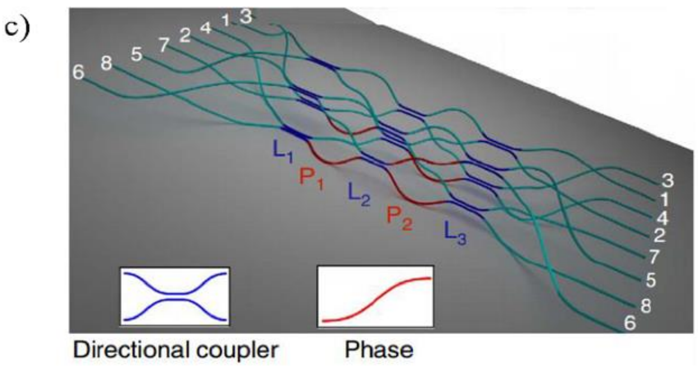

(c) Schematic of a three-dimensional 8-mode interferometer written by laser beam in borosilicate glass, realizing transformations described by Fourier matrices [125].

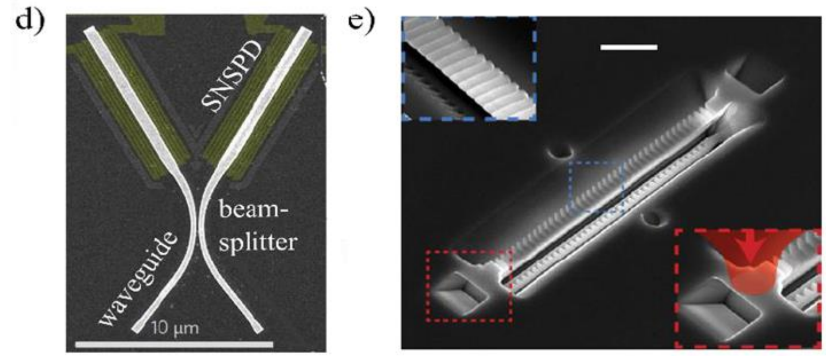

(d) A directional coupler realized with two gold plasmonic waveguides. NbN SNSPDs are integrated on the waveguides ends for realizing an on-chip two-photon interference experiment [126]. (e) SEM scan of a nanobeam YSO resonator containing Nd3+ ions for the realization of an optical quantum memory [127].

[110] H. Jin, F. M. Liu, P. Xu, J. L. Xia, M. L. Zhong, Y. Yuan, J. W. Zhou, Y. X. Gong, W. Wang, and S. N. Zhu, Phys. Rev. Lett. 113, 103601 (2014); [124] G. Calusine, A. Politi, and D. D. Awschalom, Phys. Rev. Appl. 6, 14019 (2016); [125] A. Crespi, R. Osellame, R. Ramponi, M. Bentivegna, F. Flamini, N. Spagnolo, N. Viggianiello, L. Innocenti, P. Mataloni, and F. Sciarrino, Nat. Commun. 7, 10469 (2016); [126] R. W. Heeres, L. P. Kouwenhoven, and V. Zwiller, Nat. Nanotechnol. 8, 719 (2013); [127] T. Zhong, J. M. Kindem, E. Miyazono, and A. Faraon, Nat. Commun. 6, 8206 (2015)

Performance of waveguide-based SSPD as a mixer for heterodyne spectroscopy: sensitivity is very close to the quantum limit

Power at IF versus photon flux from local oscillator

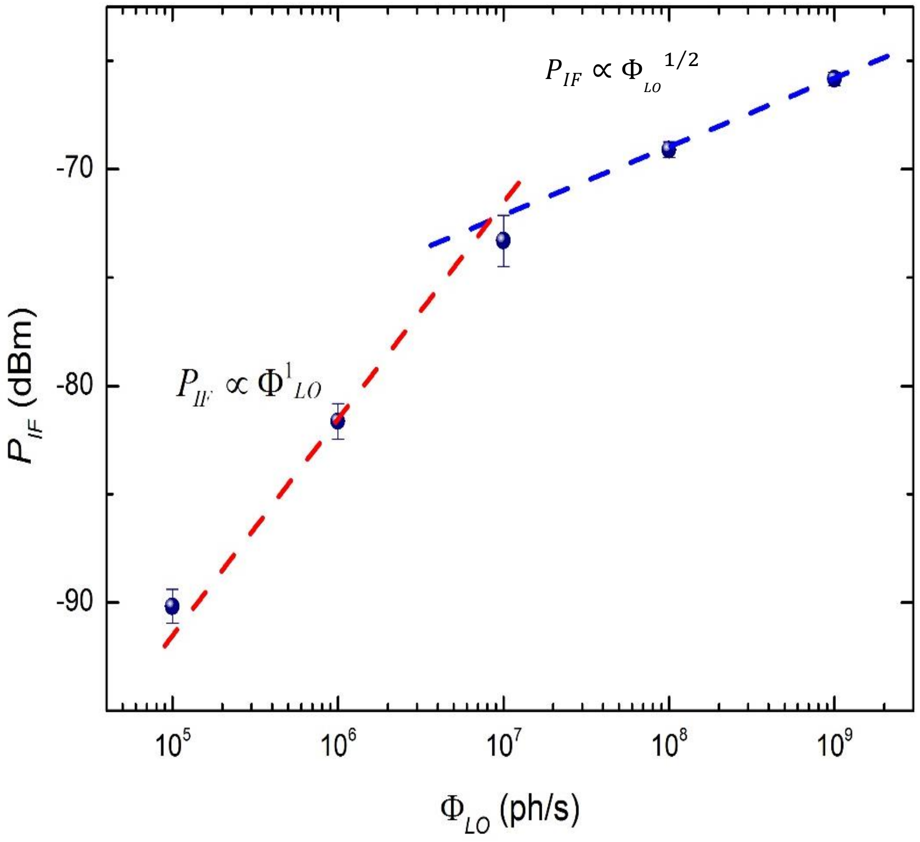

The minimum resolved energy versus photon flux from local oscillator

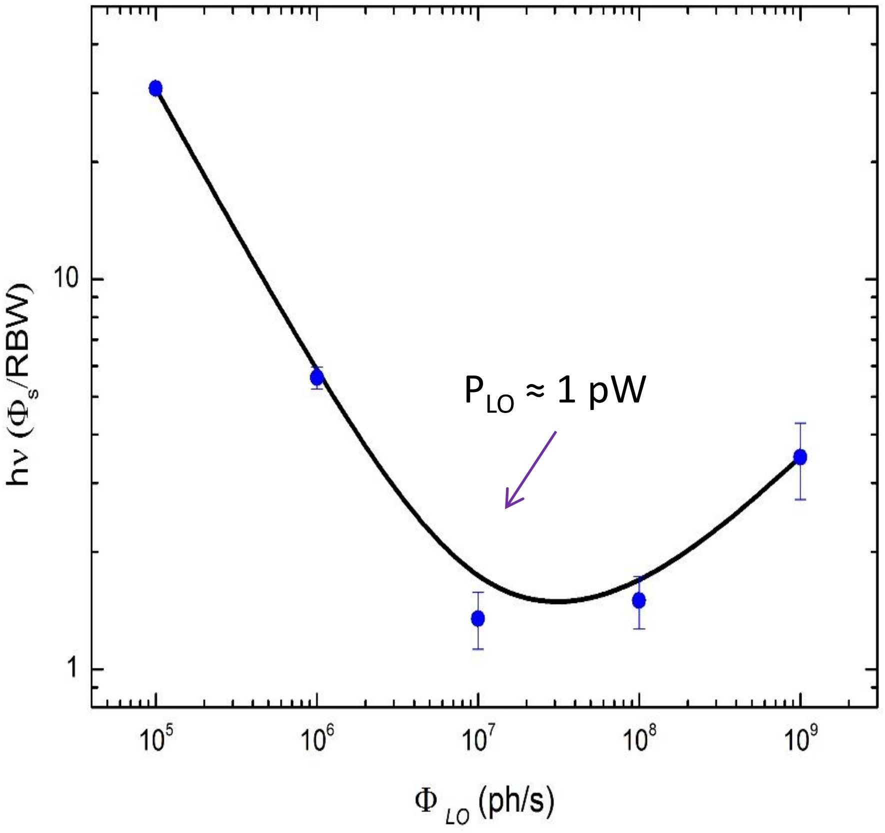

Time resolution of WSSPD

Timing jitter

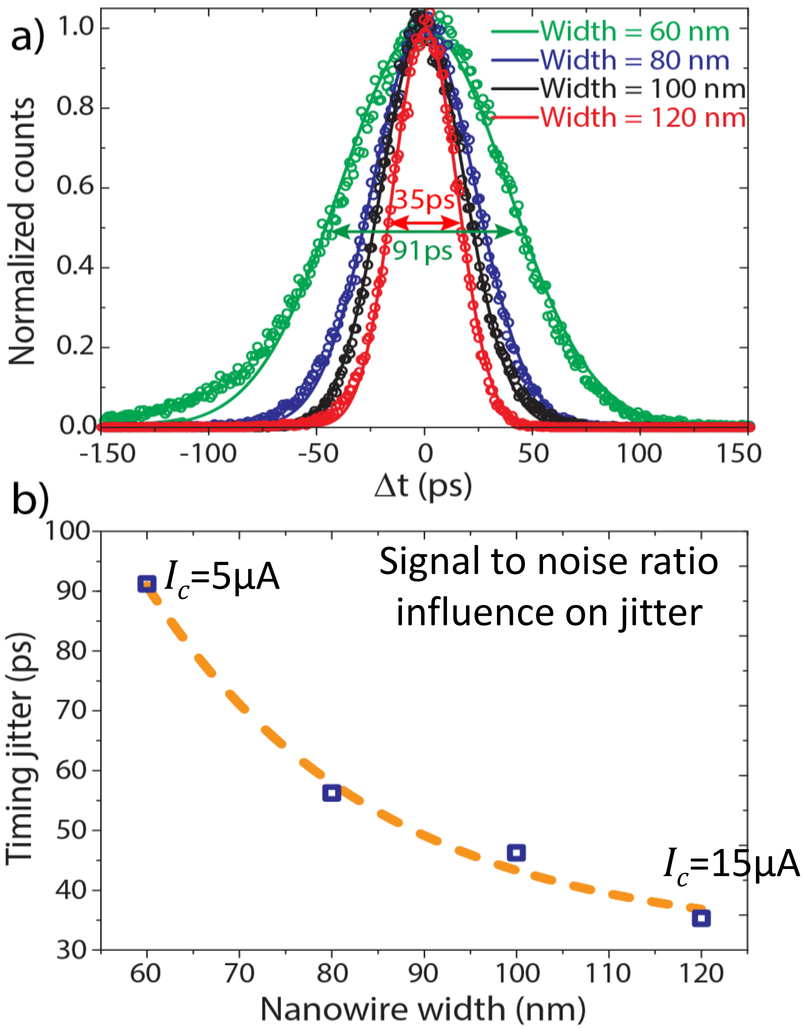

Decay time

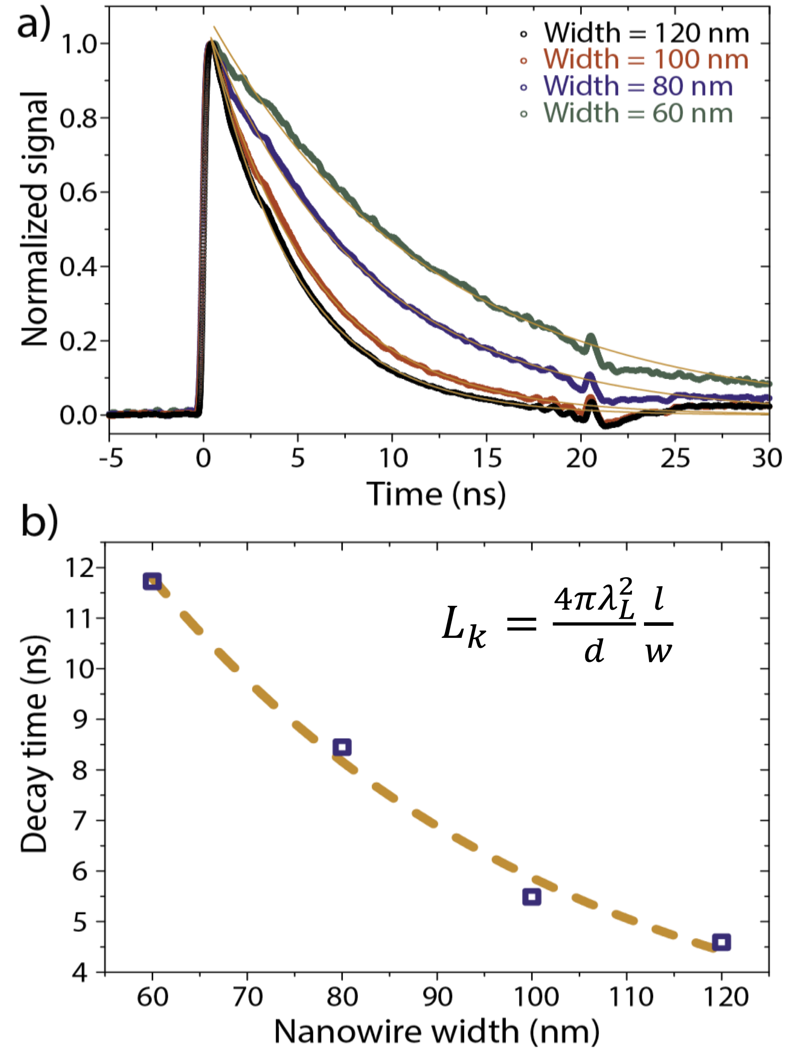

O. Kahl, S. Ferrari, V. Kovalyuk, G. N. Goltsman, A. Korneev, and W. H. P. Pernice, “Waveguide integrated superconducting single-photon detectors with high internal quantum efficiency at telecom wavelengths.,” *Sci. Rep.*, vol. 5, no. February, p. 10941, 2015.

Historical Introduction: ***Can we observe an interference between two photons originated from two different sources?***

✓ According to a famous statement by Paul Dirac[1] (1958), **no:**

".. .each photon interferes only with itself. Interference between different photons never occurs. "

✓ However, in 1967, Pfleegor and Mandel[2] have observed interference with two independent light beams with the light intensity being so low that the mean interval between photons was great compared with their transit time through the apparatus. In other words, there was a high probability that one photon was absorbed sometime before the next one was emitted by one or the other source.

1 P. A. M. Dirac, Quantum mechanics {Oxford University Press, London, 1958), 4th ed. , Chap. I, p. 9.
2 R.L. Pfleegor and L. Mandel, Phys. Rev., V. 159, No. 5, 1084 (1967).

Historical Introduction: ***Can we observe an interference between two photons originated from two different sources?***

✓ An explanation of the experiment was provided a year later by L. de Broglie and J.A. e Silva[3]:

- A photon coming from one laser or the other and arriving in the interference zone is by the superposition of the waves emitted by the two lasers, and it is for this reason that it is impossible to know in which of the two lasers it was born.
- In short, it is not the photons but the electromagnetic waves that produce the interferences; the part played by the photons, which is important, is only to permit one to detect the interferences by the manner in which they are statistically distributed in the zone where these interferences exist.

1 P. A. M. Dirac, Quantum mechanics {Oxford University Press, London, 1958), 4th ed. , Chap. I, p. 9.
2 R.L. Pfleegor and L. Mandel, Phys. Rev., V. 159, No. 5, 1084 (1967).
3 L. De Broglie, J.A. e Silva, Phys. Rev., V. 172, No. 5, 1284, (1968).

Measured data for C-band

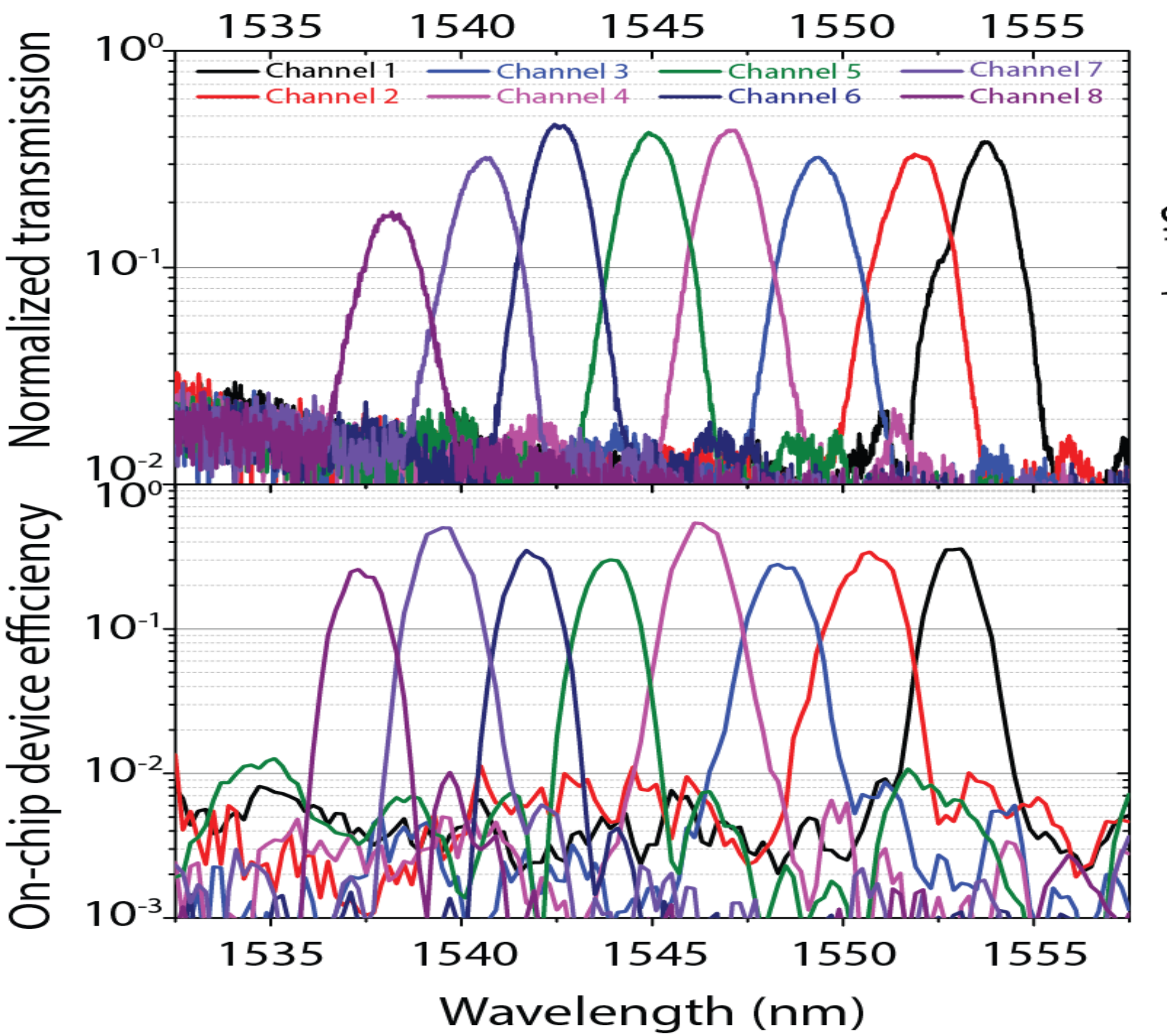

O. Kahl, S. Ferrari, V. Kovalyuk, A. Vetter, C. Nebel, A. Korneev, G. Goltsman, and W. Pernice, "Spectrally resolved imaging with hybrid superconducting - nanophotonic circuits," *ArXiv*, 2016.

SSPD as a photon counting mixer: to operation principle

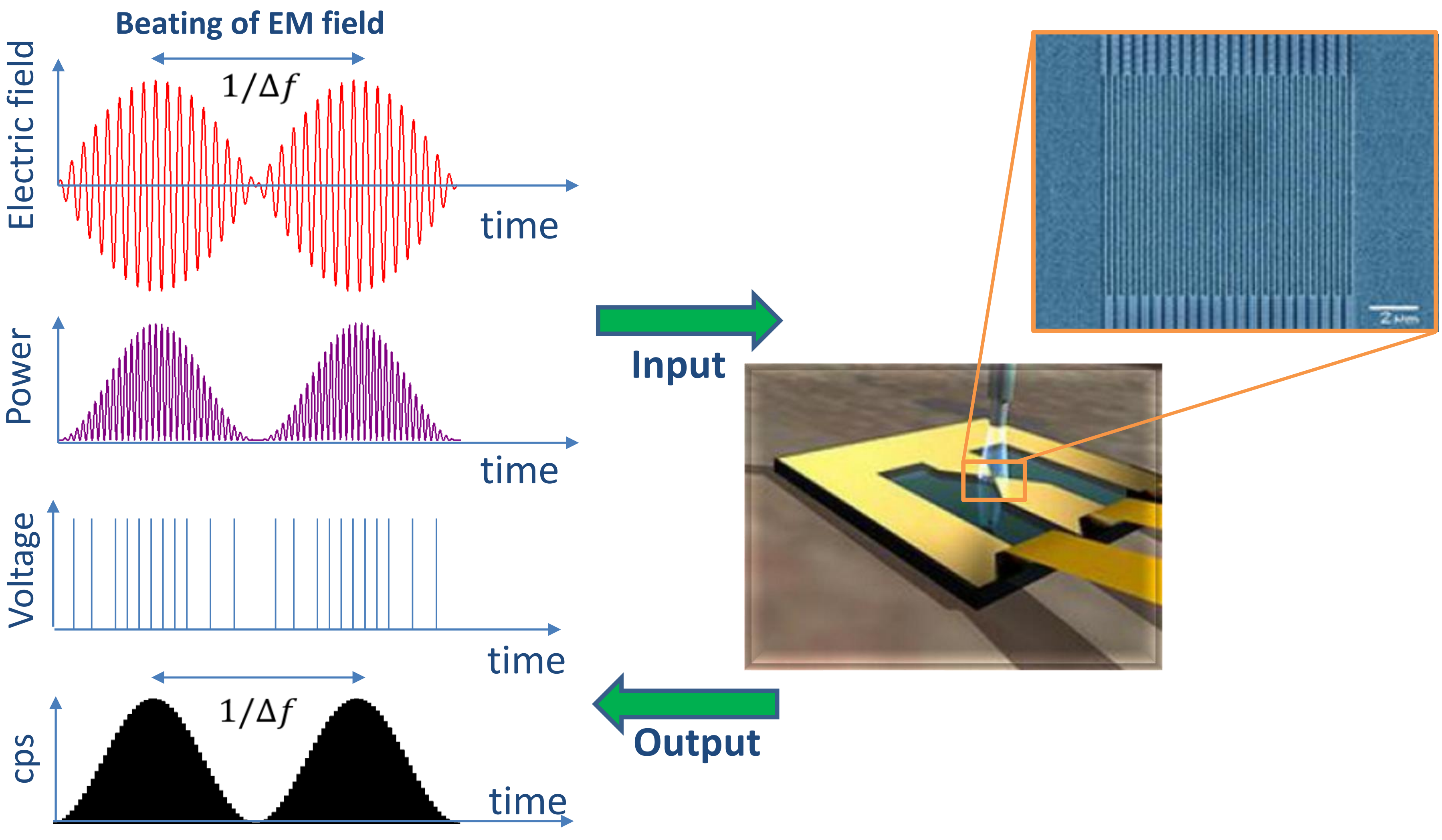

Counts per second oscillation versus time